

TM-82502  
~~N83-15335~~



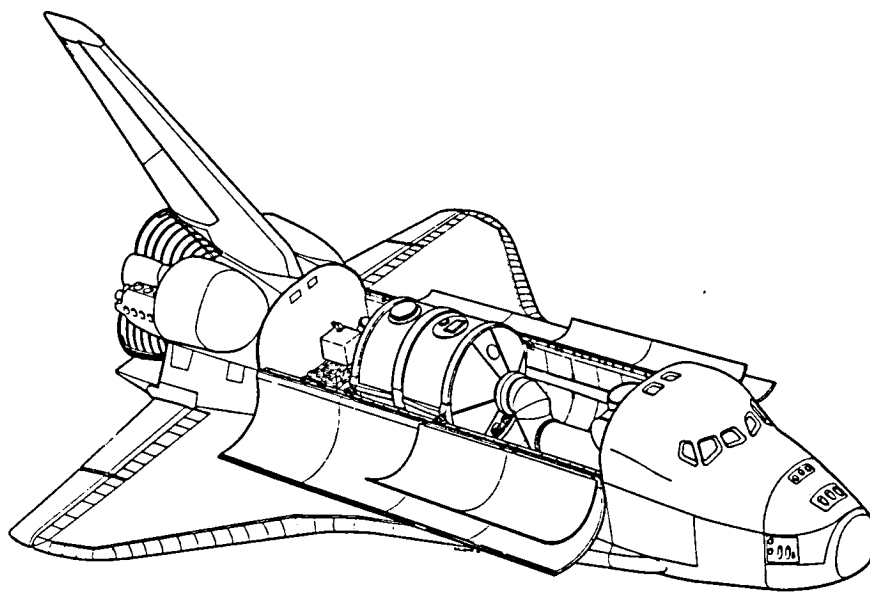
National Aeronautics and  
Space Administration

NASA-TM-82502 19830007064

NASA TM-82502

George C. Marshall Space Flight Center  
Marshall Space Flight Center, Alabama 35812

# Spacelab Mission 3 Experiment Descriptions



Edited by C. Kelly Hill  
Space Science Laboratory  
November 1982

LIBRARY COPY

MAY 9 1983

LANGLEY RESEARCH CENTER  
LIBRARY, NASA  
HAMPSHIRE, VIRGINIA



|  |  |  |  |   |                   |
|--|--|--|--|---|-------------------|
| 1. REPORT NO.<br>NASA TM- 82502  |  | 2. GOVERNMENT ACCESSION NO.                          |  | 3. RECIPIENT'S CATALOG NO.                                  |                   |
| 4. TITLE AND SUBTITLE<br>Spacelab Mission 3 Experiment Descriptions  |  |  |  | 5. REPORT DATE<br>November 1982                             |                   |
|  |  |  |  | 6. PERFORMING ORGANIZATION CODE                             |                   |
| 7. AUTHOR(S)<br>Edited by C. Kelly Hill  |  |  |  | 8. PERFORMING ORGANIZATION REPORT #                         |                   |
| 9. PERFORMING ORGANIZATION NAME AND ADDRESS<br>George C. Marshall Space Flight Center<br>Marshall Space Flight Center, Alabama 35812   |  |  |  | 10. WORK UNIT NO.   |                   |
|  |  |  |  | 11. CONTRACT OR GRANT NO.                                   |                   |
| 12. SPONSORING AGENCY NAME AND ADDRESS<br>National Aeronautics and Space Administration<br>Washington, D.C. 20546  |  |  |  | 13. TYPE OF REPORT & PERIOD COVERED<br>Technical Memorandum |                   |
|  |  |  |  | 14. SPONSORING AGENCY CODE                                  |                   |
| 15. SUPPLEMENTARY NOTES<br>Prepared by Space Sciences Laboratory, Science and Engineering  |  |  |  |   |                   |
| 16. ABSTRACT<br><p>The Spacelab 3 Mission is the first operational flight of Spacelab aboard the Shuttle Transportation System. The primary objectives of this mission are to conduct application, science, and technology experimentation that requires the low gravity environment of Earth orbit and an extended-duration, stable vehicle attitude with emphasis on materials processing. This document provides descriptions of the experiments to be performed during the Spacelab 3 Mission.</p> |  |  |  |   |                   |
| 17. KEY WORDS<br>Spacelab 3 Mission<br>Experiments<br>Materials Processing<br>Life Sciences<br>Environmental Observations<br>Astrophysics  |  |  | 18. DISTRIBUTION STATEMENT<br><br>Unclassified - Unlimited<br><i>C. Kelly Hill</i> |   |                   |
| 19. SECURITY CLASSIF. (of this report)<br>Unclassified   |  | 20. SECURITY CLASSIF. (of this page)<br>Unclassified |  | 21. NO. OF PAGES<br>50                                      | 22. PRICE<br>NTIS |

N83-15335 #



## FOREWORD

Spacelab 3 is the third in a series of modular orbiting laboratories to be undertaken in the 1980's. Spacelab is being developed by the European Space Agency (ESA) for the National Aeronautics and Space Administration (NASA). It will be flown into space by the Space Transportation System which is being developed by NASA. The general Spacelab modules consist of an unpressurized experiment support structure and pressurized modules which can be arranged in several combinations within the payload bay of the Space Shuttle Orbiter. The Spacelab Mission 3 configuration is shown in Figure 1.

The Spacelab 3 Mission is the first operational flight of Spacelab. The primary objective of the mission is to conduct applications, science, and technology experimentation requiring the low-gravity environment of Earth orbit and extended-duration stable vehicle altitude with emphasis on environmental observations and materials processing. Overall responsibility for all NASA Spacelab and attached payload missions has been assigned to the Spacelab Flight Division within the Office of Space Science and Applications (OSSA) at NASA Headquarters. The Marshall Space Flight Center (MSFC) has been assigned as the mission management center for the third Spacelab mission. Mr. John Theon of the NASA Headquarters OSSA has been designated the Program Scientist for Spacelab 3, and Dr. George H. Fichtl of MSFC has been selected as the Spacelab 3 Mission Scientist. Mr. Sterling Smith of the NASA Headquarters OSSA is the Program Manager, and Mr. Joseph Cremin of MSFC is the Mission Manager for Spacelab 3. The Spacelab 3 Mission is a low-gravity mission and primarily consists of experiments in disciplines that are within the OSSA and OAST.

Spacelab 3 is scheduled to be launched from the Kennedy Space Center (KSC) in the late 1984 timeframe, with a mission duration planned for 7 days. An orbital altitude of approximately 400 km will be achieved with an inclination of 57 degrees. Subsequent to the Spacelab 3 on-orbit activities, the Shuttle will land at KSC.

Payload Specialists (PS's) will be used on-orbit to conduct the scientific investigations. They will be selected and trained by the Spacelab 3 Principal Investigators (PI's) and facility developers. PS backups will also be selected; if not needed to fill a prime PS position on-orbit, they will then support the mission via the Payload Operational Control Center (POCC). The mission payload crew consists of the selected PS's and assigned Mission Specialists (MS's). The flight crew, consisting of a commander and co-pilot, is charged with operation of the Shuttle Orbiter. The MS's will be responsible for the interface between the Spacelab payload and the Shuttle Orbiter.

Twelve investigations have been selected to fly aboard the Spacelab 3 Mission. Of these, ten originate from the United States, one from India, and one from France (reimbursible).

The experiments represent a total of five different disciplines, including materials processing in space, environmental observations, life sciences, astrophysics, and technology research. Table 1 lists the experiments by discipline, experiment location on Spacelab, title, principal investigator, and sponsoring institution. A list of co-investigators, many of whom were also instrumental in the writing of the experiment descriptions, is provided in the appendix.

Nine of the experiments are located in the module, two are located on the Experiment Support Structure (ESS) in the payload bay, and one is in the mid-deck. The physical locations of these experiments are shown in Figures 2, 3, and 4.

The module experiments on Spacelab 3 require the planned low-gravity environment. For example, in the materials processing discipline, mercuric iodide crystals will be grown in the Vapor Crystal Growth System (VCGS) to obtain higher quality crystalline structure by taking advantage of diffusion-controlled

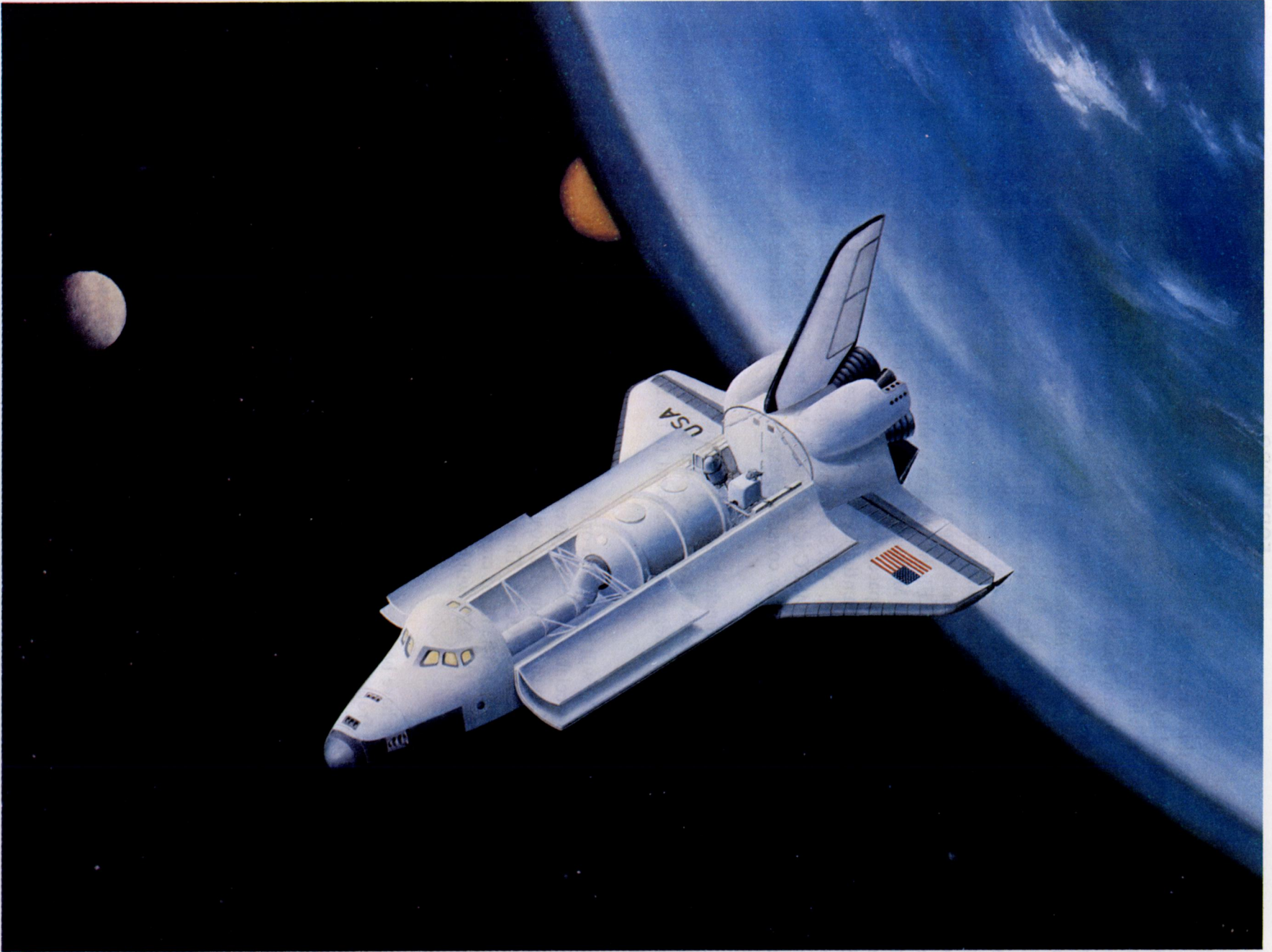


Figure 1. Spacelab Mission 3.

TABLE 1. LIST OF SPACELAB 3 EXPERIMENTS

| Discipline                    | Experiment Location In Spacelab   | Title   | Principal Investigator/Institution                                    |
|-------------------------------|-----------------------------------|---|---|
| Materials Processing in Space | Module                            | Fluid Experiment System (FES)   | Dr. R. Lal, Alabama A&M University                                    |
|                               | Module                            | Vapor Crystal Growth System (VCGS)  | Mr. W. Schneppe, EG&G, Santa Barbara                                  |
|                               | Module                            | Mercuric Iodide Crystal Growth (MICG) (Reimbursable)  | Dr. R. Cadoret, CNES  |
| Technology                    | Module                            | Drop Dynamics Module (DDM)  | Dr. T. G. Wang, Jet Propulsion Laboratory                             |
| Environmental Observations    | ESS*                              | Atmospheric Trace Molecules Spectroscopy (ATMOS)  | Dr. C. B. Farmer, California Institute of Technology                  |
|                               | Module                            | Geophysical Fluid Flow Cell (GFFC)  | Dr. J. Hart, University of Colorado                                   |
| Life Sciences                 | Module                            | Ames Research Center Life Sciences Payload Research Animal Holding Facility – Verification Test (RAHF-VT)<br>Dynamic Environment Measurement System (DEMS)<br>Biotelemetry System (BTS) | Dr. J. Tremor, Facility Science Manager, NASA Ames Research Center    |
|                               | Mid-Deck (See Module Experiments) | JSC Life Sciences Payload Urine Monitoring (UMS)  | Dr. H. Schneider, Facility Science Manager, NASA Johnson Space Center |
| Astrophysics                  | ESS                               | Ionization States of Solar and Galactic Cosmic Ray Heavy Nuclei (IONS; also ANURAHDA)   | Dr. S. Biswas, Tata Institute of Fundamental Research, India          |

\*Experiment Support Structure

NOTES:

1. RACK ARRANGEMENTS SHOWN INDICATE VOLUME ALLOCATIONS NOT FRONT PANEL CONFIGURATIONS.

⚠ EPSP ACCESS PANEL FOR CLOSEOUT ONLY. NO EPSP IN RACK

LEGEND



MDE



MPE



NFE

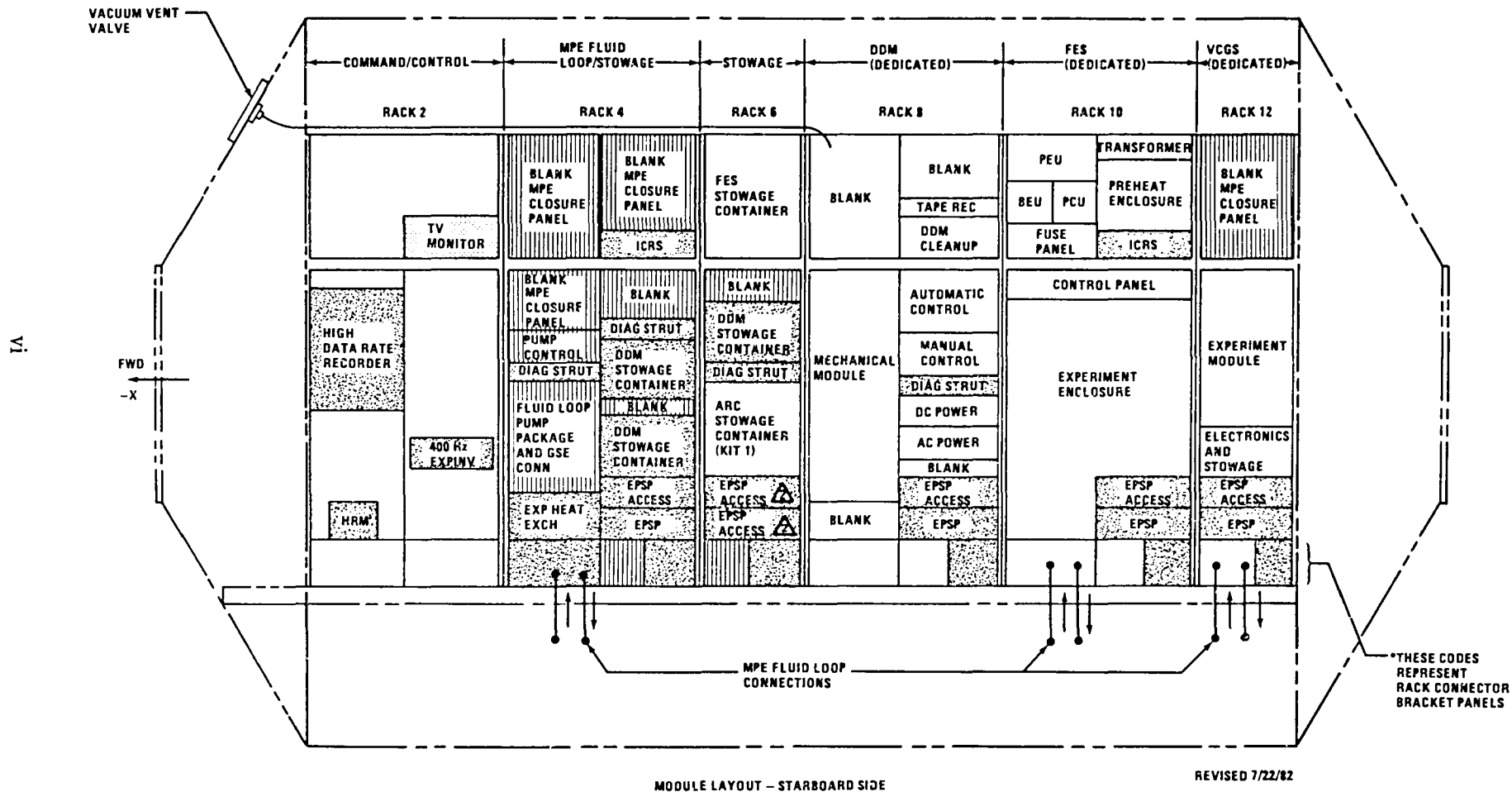


Figure 2. SL-3 module layout (starboard side). (See Table 1 for experiment acronym definition.)



NOTES:

1. RACK ARRANGEMENTS SHOWN INDICATE VOLUME ALLOCATIONS NOT FRONT PANEL CONFIGURATIONS.

▲ EPSP ACCESS PANEL FOR CLOSEOUT ONLY. NO EPSP IN RACK

LEGEND



MDE

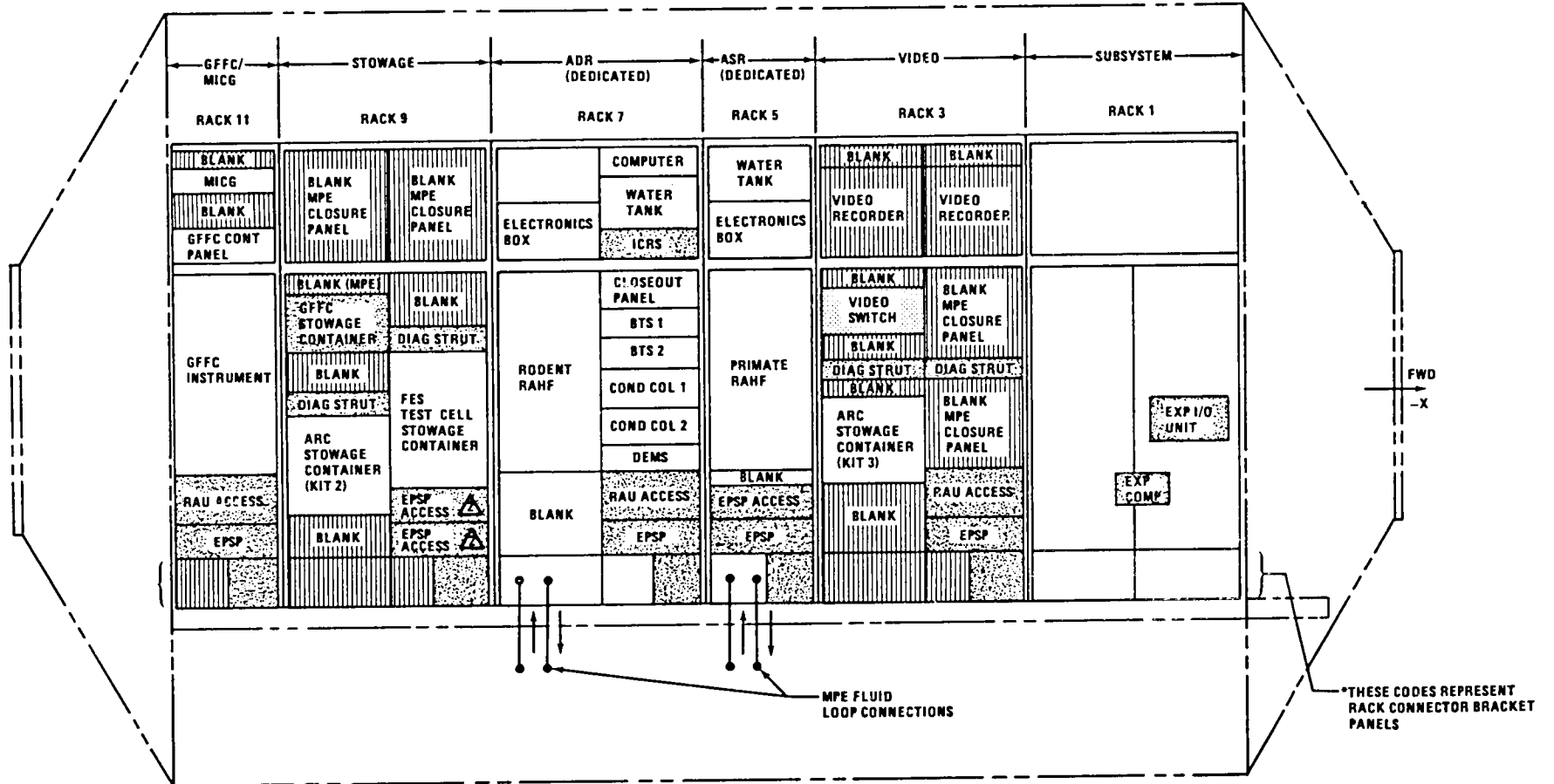


MPE



NFE

vii



MODULE LAYOUT - PORT SIDE

REVISED 7/22/82

Figure 3. SL-3 module layout (port side). (See Table 1 for experiment acronym definitions.)

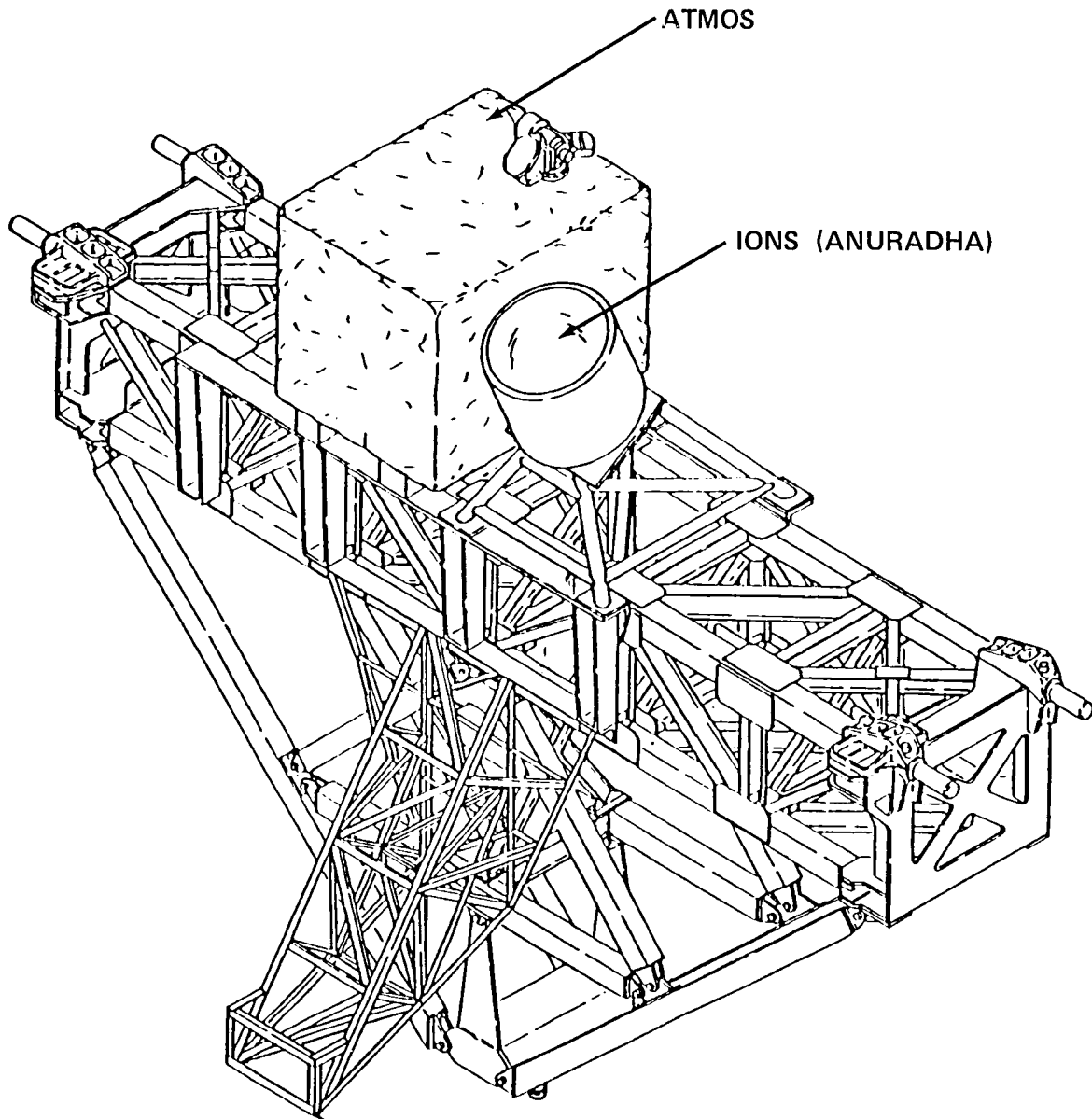


Figure 4. SL-3 experiments on ESS. (See Table 1 for acronym definitions.)

growth conditions and by avoiding the problem of strain dislocations produced by the crystal's weight, as occurs in terrestrial laboratories. Another experiment, Mercury Iodide Crystal Growth (MICG), will utilize a two-zone furnace to grow near-perfect single crystals. Further, in the Fluid Experiment System (FES), tri-glycine sulfate crystals will be grown from seed crystals via a solution process to develop a growth technique for low-gravity, characterize this growth environment, and determine effects thereof on crystal properties.

Two experiments in fluid mechanics are planned that require a low-gravity environment as well as an extended duration of stable vehicle attitude. One experiment, Dynamics of Rotating and Oscillating Free Drops (DROP), will be performed using the Drop Dynamics Module (DDM). In this experiment, basic studies on the dynamics of rotating and oscillating drops will be made with a view toward confirming specific theoretical predictions and gaining insight and direction relative to those dynamical processes not currently accessible by theory. A second fluid mechanics experiment, the Geophysical Fluid Flow Cell (GFFC), is aimed at the study of the essential fluid mechanics of spherical convection processes as found in planetary atmospheres and stellar interiors. It will attempt to confirm specific theoretical predictions related to the dynamics of the solar convective zone and the Jovian atmosphere.

The life sciences experiments being conducted by NASA's Ames Research Center (ARC) and Johnson Space Center (JSC) will evaluate the performance of specially designed equipment and facilities for use in a low-gravity environment. These should optimize the experimental capabilities for life sciences research in future Spacelab missions. Both human and animal subjects will be used in a variety of measurement and observation activities for the acquisition of physiological, behavioral, and morphological data for later analysis and studies.

One of the ESS-mounted experiments, the Atmospheric Trace Molecule Spectroscopy (ATMOS), will make observations of trace gases and constituents during Earth sunrises and sunsets. The measurements acquired by the ATMOS will help provide a global mapping of trace molecules in our atmosphere. These global data will play a key role relative to our understanding of radiative, chemical, and dynamic processes of the stratosphere and mesosphere.

Another experiment on the ESS (Figure VII-1), Ionization States of Solar and Galactic Cosmic Ray Heavy Nuclei (IONS; also known as ANURADHA), is designed to make direct measurements of the charge state of low-energy heavy ions which are crucial to the understanding of new-particle phenomena observed on Skylab and other satellites. Information on the ionization states of solar heavy nuclei that may be provided by this experiment is of immediate interest in the understanding of the acceleration and confinement of energetic nuclei in the Sun.

Spacelab 3 is the first mission in which a low-gravity environment will be strictly maintained in orbit. Furthermore, the vehicle will be operated in a gravity gradient flight mode during the full on-orbit mission duration; and drift will be carefully controlled. These conditions are unique but necessary for conducting most of the experiments on this multidisciplinary mission.



## TABLE OF CONTENTS

|   | Page |
|---|------|
| MODULE EXPERIMENTS .....  | 1    |
| I. Materials Processing in Space. ....  | 3    |
| A. Solution Growth of Crystals in Zero Gravity (Ravindra B. Lal). ....                                    | 3    |
| B. Mercuric Iodide (HgI <sub>2</sub> ) Crystal Growth for Nuclear Detectors<br>(Wayne F. Schnepfle) ..... | 5    |
| C. Mercuric Iodide Crystal Growth (R. Cadoret) .....  | 9    |
| II. Dynamics of Rotating and Oscillating Free Drops (T. G. Wang) .....                                    | 13   |
| III. Geophysical Fluid Flow Cell Experiment (John E. Hart) .....  | 17   |
| IV. Ames Research Center Life Sciences Payload<br>(Paul X. Callahan and John W. Tremor) .....             | 21   |
| A. Research Animal Holding Facilities (Primate and Rodents)<br>Verification Test (RAHF-VT) .....          | 21   |
| B. Dynamic Environment Measurement System and Biotelemetry<br>System Investigations .....                 | 25   |
| V. JSC Life Sciences Payload (H. Schneider) .....   | 25   |
| Urine Monitoring Investigation .....  | 25   |
| EXPERIMENT SUPPORT STRUCTURE EXPERIMENTS .....  | 27   |
| VI. Atmospheric Trace Molecule Spectroscopy (C. B. Farmer) .....  | 29   |
| VII. Studies of the Ionization States of Solar and Galactic Cosmic Ray<br>Heavy Nuclei (S. Biswas) .....  | 35   |
| Appendix .....  | 39   |

## LIST OF ILLUSTRATIONS

| Figure | Title  | Page |
|--------|--|------|
| I-1.   | FES rack assembly .....  | 4    |
| I-2.   | FES test cell layout.....  | 6    |
| I-3.   | VCGS experiment module elements .....  | 7    |
| I-4.   | VCGS rack assembly.....  | 8    |
| I-5.   | MICG experiment .....  | 10   |
| I-6.   | Block diagram of Mercury Iodide Crystal Growth Experiment .....  | 11   |
| II-1.  | Drop dynamics module integrated double rack .....  | 15   |
| III-1. | Geometry of the GFFC rotating spherical shell experiment .....   | 18   |
| III-2. | Geophysical fluid flow cell .....  | 19   |
| IV-1.  | Ames double rack (ADR) and Ames single rack (ASR); representation of RAHF-VT, DEMS, and BTS .....  | 22   |
| V-1.   | Urine monitoring system on-orbit configuration.....  | 26   |
| VI-1.  | ATMOS: interferometer optical path .....   | 32   |
| VI-2.  | ATMOS observational method for a typical sunset occultation, showing the Orbiter as it views solar radiation [O] passing through successively lower layers of the stratosphere ..... | 32   |
| VI-3.  | Expected detectability of several of the important stratospheric species by ATMOS .....  | 33   |
| VII-1. | Sketch of the IONS (ANURADHA) detector assembly (sectional view) .....   | 37   |

## LIST OF TABLES

| Table | Title   | Page |
|-------|---|------|
| II-1. | Drop Science Requirements and Parameters .....  | 16   |
| VI-1. | ATMOS Instrument Characteristics.....   | 31   |
| VI-2. | Transmission Regions for ATMOS Optical Filters Showing Principal Species to Be Measured ..... | 33   |

## **MODULE EXPERIMENTS**





# I. MATERIALS PROCESSING IN SPACE

## A. SOLUTION GROWTH OF CRYSTALS IN ZERO GRAVITY

Ravindra B. Lal  
Alabama A&M University

A series of experiments will be performed in which triglycine sulfate (TGS) crystals will be grown by a low-temperature solution growth technique in the microgravity environment of the orbital Spacelab. The objectives are:

- 1) To develop a technique for solution crystal growth in a low-gravity environment;
- 2) To characterize the growth environment provided by an orbiting spacecraft and to determine the influence of the environment on the growth behavior;
- 3) To determine how growth in a low-g environment influences the properties of a resultant TGS crystal.

Triglycine sulfate (TGS) crystals will be grown in the Fluid Experiment System (FES) facility on Spacelab 3 by slowly extracting heat at a controlled rate through a seed crystal of TGS suspended on an insulated sting in a saturated solution of TGS. The FES rack assembly designed for SL-3 is shown in Figure I-1, and a detailed view of the test cell layout is presented in Figure I-2. Variations in the liquid density, solution concentration, and temperature around the growing crystal will be studied using a variety of techniques, such as schlieren, shadowgraph, and interferometric measurements. Growth in Earth gravity will also be studied by the same optical techniques, and in both cases the resulting crystalline features will be compared and correlated with the growth conditions.

Schlieren and shadowgraph images of crystals growing from solutions in Earth gravity show massive convective flow because of thermal and concentration gradients as the solute is incorporated into the crystal. Generally, this is controlled by gently stirring the solution to maintain uniform growth conditions. However, this uniformity can only be approximated; and small-scale inhomogeneities always exist which adversely affect the growth of the crystal. In a microgravity environment, it should be possible to significantly reduce convective flows and thus establish a diffusion-controlled transport of the solute to the interface. By extracting heat from the crystal in a controlled manner, it should be possible to maintain saturation at the growth interface. This should allow a slow but very uniform growth, resulting in a higher degree of crystal perfection. Also, the growth rates for different crystallographic axes should be determined unambiguously and can be compared with existing crystal growth theories. In addition, TGS crystals have practical applications as infrared detectors whose performance might be improved by increased perfection.

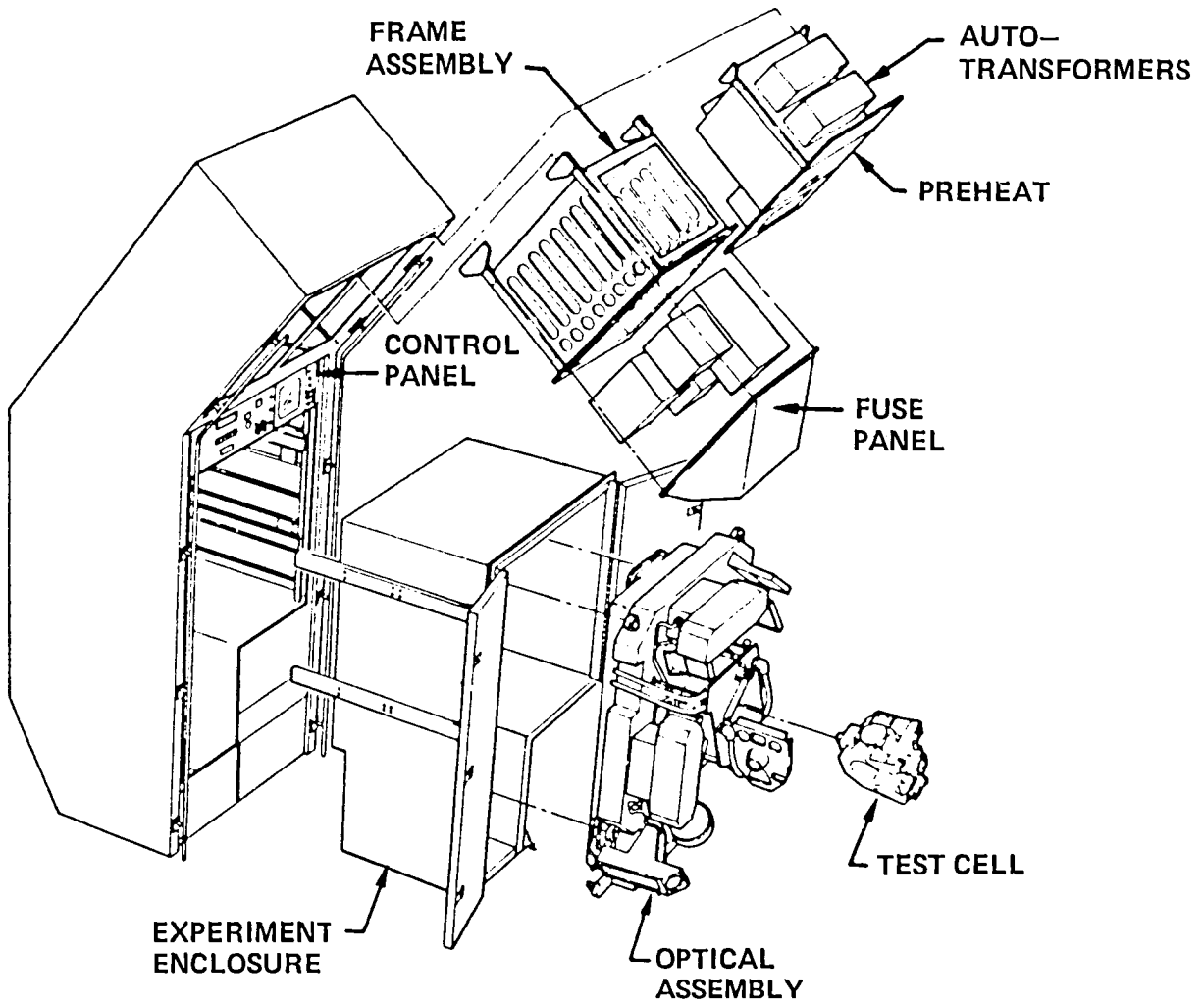


Figure I-1. FES rack assembly.

## B. MERCURIC IODIDE ( $\text{HgI}_2$ ) GROWTH FOR NUCLEAR DETECTORS

Wayne F. Schneppe  
EG&G, Inc., Santa Barbara Operations  
Goleta, California

The purpose of this investigation is to grow more-perfect mercuric iodide crystals in a low-gravity environment by taking advantage of diffusion-controlled growth conditions and by avoiding the problem of strain dislocations produced by the crystal's weight. This crystal has considerable practical importance as a sensitive gamma-ray detector and energy spectrometer that can operate at ambient temperature, as compared to presently available detectors that must be cooled to near liquid nitrogen temperatures. However, the performance of mercuric iodide crystals only rarely approaches the expected performance, presumably because some of the free electrical charges produced within the crystal are not collected at the electrodes, but instead remain trapped or immobilized at crystal defects. An efficient high atomic number semiconductor detector capable of operating at room temperature utilizing single  $\text{HgI}_2$  crystals offers a greater potential than existing detector technology.

These crystals will be grown by vaporization and recondensation at approximately  $120^\circ\text{C}$  in a specially designed furnace located in the Vapor Crystal Growth System (VCGS) (Fig. I-3). The VCGS rack assembly designed for SL-3 is shown in Figure I-4. Provisions will be made to reverse the growth procedure if polycrystalline growth begins, which is a common problem in growing this crystal on the ground. Extensive experiments will be conducted prior to flight to optimize the growth process, to establish the best performance that can be obtained in the terrestrial laboratory, and to provide a basis for comparison with the low-gravity results.

There is good reason to believe that the growth of this crystal can be improved in a low-gravity environment. The low level of gravity-driven convection reduces fluctuations in the vapor density and temperature in the vicinity of the seed crystal. This better-controlled environment is conducive to uniform growth with far fewer defects, as demonstrated by Wiedemeier\* on Skylab. Secondly, this crystal structure is a layer-type with weak bonding between slip planes. It is suggested that the high dislocation densities and strain fields observed in the terrestrially grown crystal probably originate from the weight of the crystal as it is supported during growth.

It is thus anticipated that the mercuric iodide crystals grown in space will have lower defect densities and will exhibit better performance than the best mercuric iodide grown terrestrially. This could help establish the inherent performance of this crystal and may possibly lead to production of a limited number of these crystals in space for use as experimental nuclear radiation detectors.

---

\*Vol. 1 Proceedings, Third Space Processing Symposium, Skylab Results, (NASA Report), April 30-May 1, 1974.

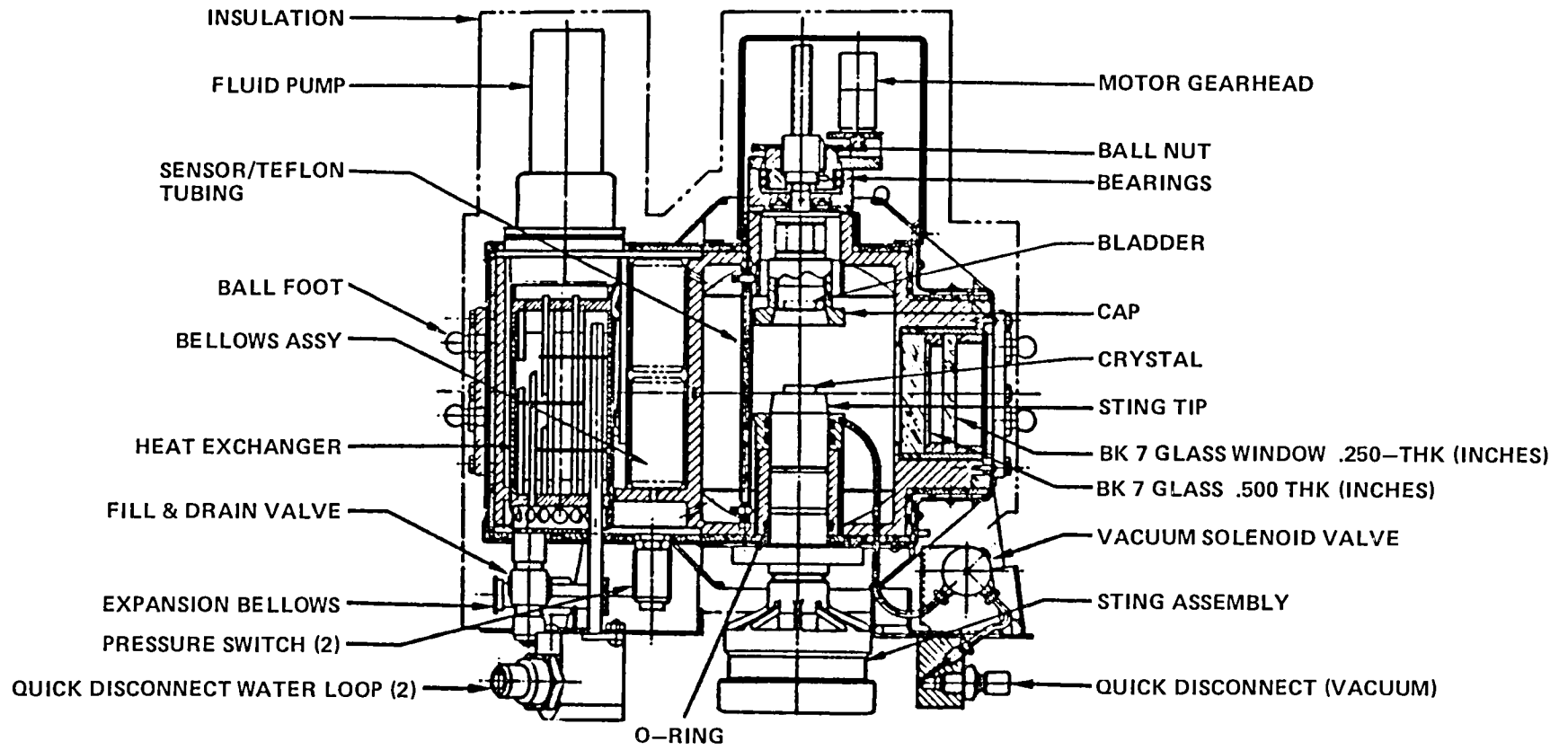


Figure I-2. FES test cell layout.

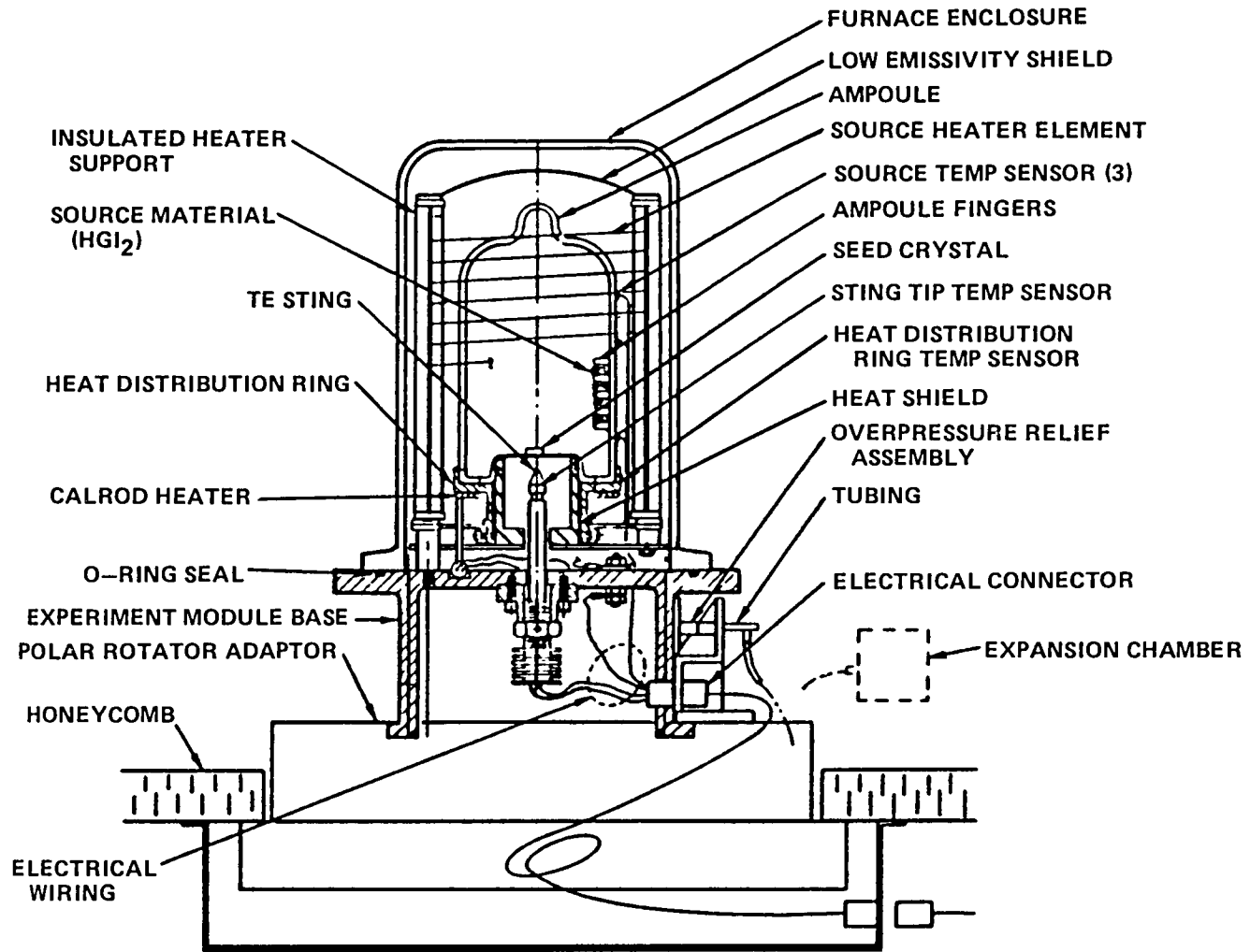


Figure I-3. VCGS experiment module elements.

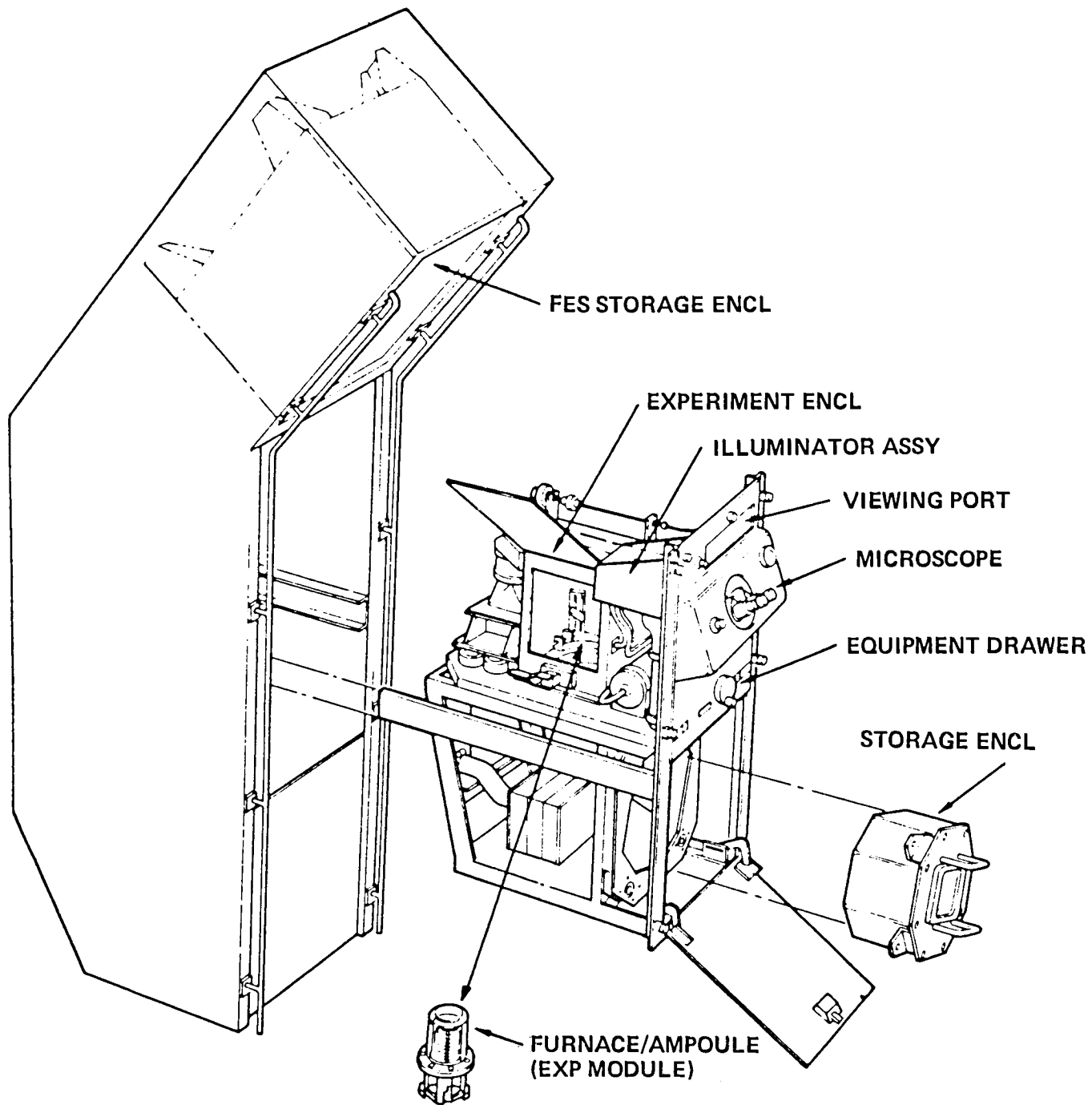


Figure I-4. VCGS rack assembly.

## C. MERCURY IODIDE CRYSTAL GROWTH

R. Cadoret

Laboratoire d'Crystallographie Het et de Physique

The purpose of the Mercury Iodide Crystal Growth (MICG) experiment is the growth of near-perfect single crystals of Mercury Iodide ( $\text{HgI}_2$ ) in a microgravity environment which will decrease the convection effects on crystal growth. Evaporation and condensation are the only transformations involved in this experiment. To accomplish these objectives, a two-zone furnace will be used in which two sensors collect the temperature data (one in each zone).

Figure I-5 provides a view of the oven and electronics (with and without the front panel) mounted on a rail system to the rack. It is not proposed that any operations requiring the crew to manually move any item are needed. The frontal view indicates the three vertically aligned fuses on the electronics front panel. Additionally a green light is provided to indicate that the power supply is connected. Beneath the green light is a three position lever switch, which allows manual operations. A cross-sectional view of the MICG showing the two-zone furnace configuration is depicted in Figure I-6.

Normal operations of the experiment are performed by the experiment computer. The sequence of experiment operation over the mission and the duration of the single operation is approximately 100 hours. The computer switches the experiment on through programmed instructions. During the operation of the experiment, the computer monitors the power supply status and the temperature difference between the two zones within the oven. A light, and possibly an audible tone from the Command and Data Management Subsystem (CDMS) caused by either of these parameters being out-of-limits is sufficient for crew intervention. At the end of normal operations, the computer will shut the experiment down.

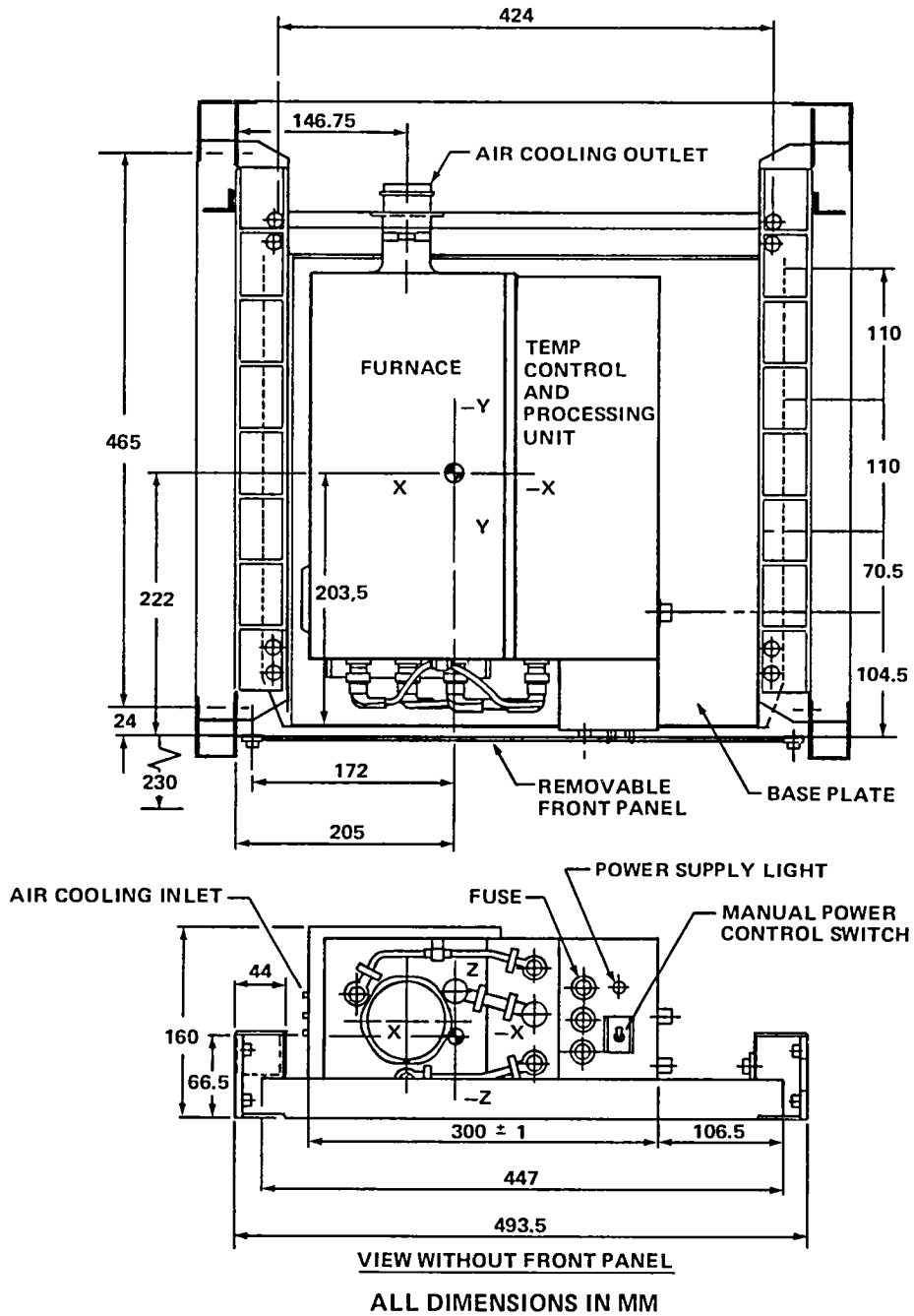
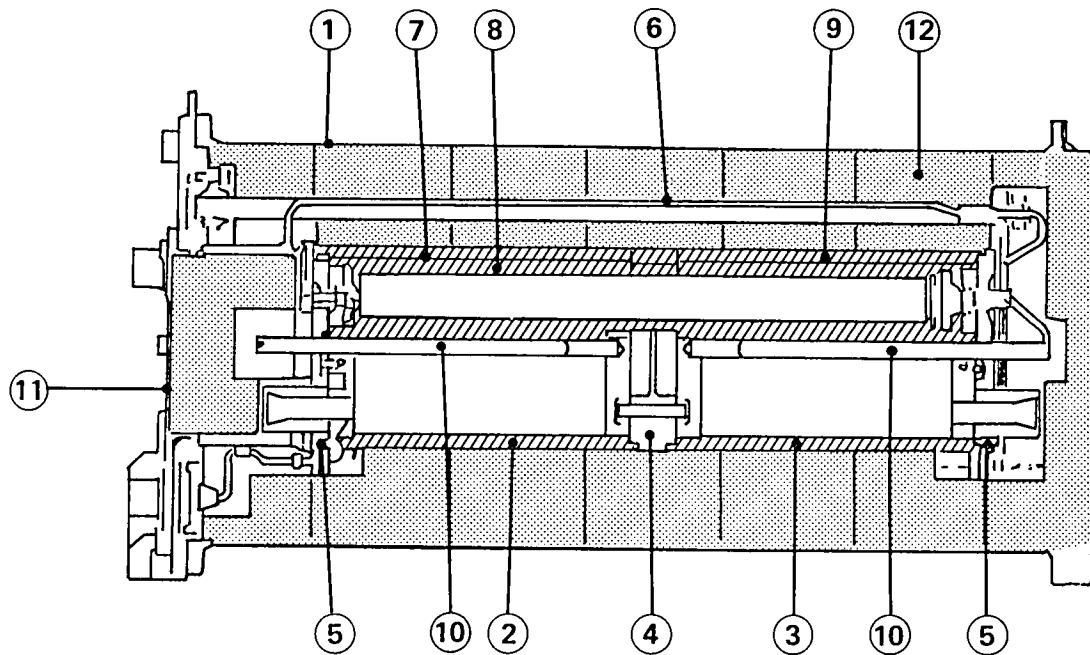


Figure I-5. MICG as viewed in the rack with and without front panel.





- |   |                       |
|---|-----------------------|
| 1. FURNACE COVERING                               | 7. CARTRIDGE          |
| 2. HEAT PIPE A                                    | 8. QUARTZ AMPOULE     |
| 3. HEAT PIPE B                                    | 9. HEATING ELEMENT    |
| 4. REFRACTOR <sup>y</sup> FOR HEAT PIPES A AND B  | 10. TEMPERATURE PROBE |
| 5. EXTERIOR REFRACTOR <sup>y</sup> FOR HEAT PIPES | 11. END CAP           |
| 6. HEAT PIPE FASTENER FOR HEAT PIPE/BASEPLATE     | 12. INSULATION        |

Figure I-6. MICG two zone furnace.



## II. DYNAMICS OF ROTATING AND OSCILLATING FREE DROPS

T. G. Wang  
Jet Propulsion Laboratory

The Dynamics of Rotating and Oscillating Free Drops (DROP) experiment is to be performed using the Drop Dynamics Module (DDM), shown in Figure II-1. The main scientific objectives of the DROP experiment are the study of the equilibrium figures of a rotating drop and the study of the large-amplitude oscillations of a liquid drop. The objective of the DROP experiment in relation to the DDM is to establish the advantages of conducting future drops and bubbles experiments in space. A complete discussion of the DROP experiment and objectives is contained in JPL Document No. 701-238, "Dynamics of Rotating and Oscillating Free Drops," Earth and Space Sciences Division, Jet Propulsion Laboratory. The DROP experiment will be subjected to continual development to ensure that the experiments are scientifically current and available.

The two component experiments (rotation and oscillation) of the DROP experiment have been chosen as the simplest experiments representative of the entire class of drop dynamics experiments. This choice has been validated by consultation with the Steering Committee of the International Colloquium on Drops and Bubbles.

The component experiment on the equilibrium shapes of a rotating liquid drop of a simple liquid is not only an important and interesting experiment in its own right, but is also the simplest gyrostatic experiment that can be performed. In later experiments, more complicated liquids can be used; bubbles can be included; and the dynamics of rotating drops can be studied. This experiment, as it now stands, is an important exercise of the module's ability to provide drop rotation and the requisite science data.

Similarly, the component experiment to observe the large-amplitude, nonlinear oscillations of a simple liquid drop is the simplest dynamic experiment that can be performed. Again, in later experiments, more complicated liquids can be used; bubbles can be included; and the non-periodic dynamics of an oscillating drop can be studied. Also, as it now stands, this experiment is an important exercise of the module's ability to provide drop oscillation and the requisite science data.

Moreover, the most complete and extensively investigated theories of liquid drops will for the first time be unambiguously tested by these experiments. Consequently, the experiments will indicate how the theories must be revised, if they must, and so will set the stage for all later experiments on liquid drops.

The detailed objectives for the rotation experiment are:

(1) Bifurcation points of a rotating drop: theory predicts the critical angular velocity at which the sequence of axisymmetric shapes becomes dynamically unstable, losing stability to a sequence of triaxial shapes. This will happen discontinuously. The experiment will determine this critical angular velocity at the bifurcation point.

(2) Nature of the instability at the bifurcation point of a rotating drop: a secular instability of the axisymmetric sequence in favor of the triaxial sequence has been predicted to occur at a second and lower critical velocity. This experiment would determine if it exists.

(3) Hysteresis of the bifurcation point of a rotating drop: because of the two critical velocities, spin-up and spin-down may manifest different bifurcation points. Another hysteresis may occur even for

small excursions of the angular velocity about a bifurcation point as a result of non-ideal conditions, such as a slight deviation from rigid-body rotation in the drop or flows in the surrounding gas.

(4) Equilibrium shapes of a rotating drop: the shapes of the axisymmetric sequence have been extensively calculated, but the shapes of the triaxial sequence have not. The shapes obtained in the experiment would be compared with the existing calculations.

(5) Oscillations of a rotating drop: the frequencies and decay constants of the free oscillations of a rotating drop have been calculated for the axisymmetric sequence. No calculations exist for the triaxial sequence. The experiment would determine frequencies/decay constraints.

The detailed objectives for the oscillation experiment are to determine the:

- (1) Frequency of large-amplitude drop oscillations;
- (2) Damping of large-amplitude drop oscillations;
- (3) Shaping of large-amplitude drop oscillations.

The preceding quantities have been predicted in computation only for the lowest mode of oscillation. The experiment will allow comparison of observed and calculated values. It should be noted, however, that, even for linear oscillations, no experiments exist that demonstrate conclusively any mode higher than the fundamental.

(4) Mode coupling in large-amplitude oscillations of a drop: the oscillations can be analyzed by computing a power spectrum from the shape oscillations determined from the film record. The resolution of each large-amplitude mode into the linear modes indicates the amplitude of each of the linear modes in the large-amplitude oscillation, or the mode coupling.

(5) Effect of internal turbulent flow on the relationship between amplitude and frequency/damping of a mode: for a sufficiently large amplitude, the velocities of the internal flows (sufficiently high Reynolds number) should cause the flows to become turbulent, a condition which could very well manifest itself as a break in the plot of the mode coupling versus amplitude. This would allow the precise onset of turbulence in a drop to be measured for the first time.

(6) Shape at the Bohr-Wheeler saddle point:<sup>1</sup> for a drop that is sufficiently deformed, the drop will not oscillate but will instead fission. The shape of the drop for an energy of the drop infinitesimally less than the lowest energy required for fission has been calculated and is known as the Bohr-Wheeler shape. The experiment will determine this energy and the Bohr-Wheeler shape.

(7) Drop fission:<sup>1</sup> the experiment will study the dynamics of drop fission in excess of the lowest energy at which fission takes place. Of particular interest are the evolution of the fission shape and the detail of pinch-off.

(8) Aperiodic motion of the drop:<sup>1</sup> the damping of even the linear oscillations of a drop has a remarkable dependence on viscosity. The time dependence of a drop shape has been predicted to become aperiodic for a sufficiently small drop (the size is dependent on the viscosity), and other interesting aperiodic behavior has been predicted. However, none of these have yet been verified.

Science requirements and parameters for the DROP experiment are summarized in Table II-1.

---

1. Not presently included as part of the baseline experiment because of the amount of attention required from the Payload Specialist.

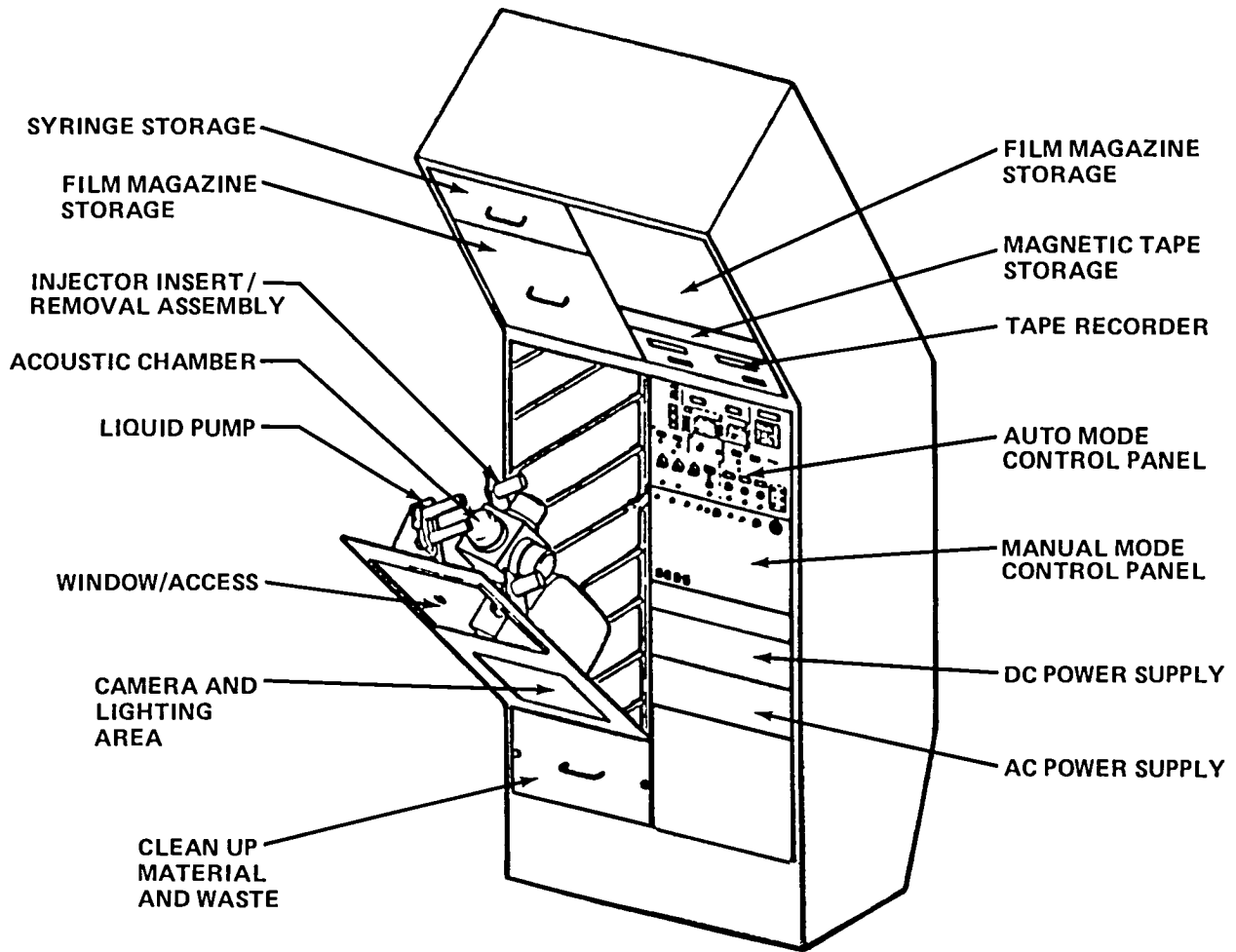


Figure II-1. Drop dynamics module integrated double rack.

TABLE II-1. DROP SCIENCE REQUIREMENTS AND PARAMETERS

I. GENERAL

A. Liquid Properties

- (1) Droplet Size - 0.3 cm to 1.5 cm in radius, stable to within 0.03 percent during the experiment
- (2) Viscosity - 1 centistoke to 1000 centistoke
- (3) Surface Tension - 10 dyne/cm to 100 dyne/cm
- (4) Transmission Coefficient - 0.3 to 1 in visible region
- (5) Index of Refraction - 1.2 to 2.0

B. Resolution

- (1) Spatial - 0.02 cm in linear dimension, 0.2 cm in internal flow (tracer particles 0.1 mm to 1 mm)
- (2) Temporal - 0.01 Hz in oscillation and rotation frequency

C. Positioning Force

- (1) Force on a 2.5 cm Diameter Drop - 0.01 dyne to 10 dyne as measured at 1.25 cm from center of the chamber
- (2) Pressure Profile - spherical to within 5 percent as measured at a radius of 1.25 cm from the chamber center

D. Temperature Stability

Surface tension and viscosity stable to within 1 percent of its value during the course of the experiment ( $\cong \pm 1^\circ\text{C}$ )

II. ROTATION

A. Rotation Velocity - 0 to 60 rad/sec, stable to within 0.1 rad/sec

B. Rotation Acceleration -  $0.01 \text{ rad/sec}^2$  to  $1 \text{ rad/sec}^2$ , stable to within  $0.01 \text{ rad/sec}^2$

III. OSCILLATION

A. Modulation Force - maximum of 10 dyne as measured at 1.25 cm from center of the chamber, stable to within 0.1 dyne

B. Modulation Frequency - 0 to 100 Hz, stable to within 0.01 Hz; linear and exponential sweep

C. Modulation Index - 0 to 100 percent, stable to within 1 percent

### III. GEOPHYSICAL FLUID FLOW CELL EXPERIMENT

John E. Hart  
University of Colorado

The primary purpose of the geophysical flow experiments is to simulate large-scale baroclinic (density-stratified) flows which occur naturally in the atmospheres of rotating planets and stars and to gain insights and obtain answers to crucial questions concerning the large-scale nonlinear mechanics of the global geophysical flows. In particular, the investigator hopes to identify those external conditions related to fluid viscosity, rotation, gravity, etc., which allow qualitatively different modes of instability or waves in the model. The investigator is trying to understand, in a geophysical context, why Jupiter and Saturn have axisymmetric cloud patterns as compared to the Sun which, as a rotating convecting body like Jupiter, seems to have a preferred orientation of large eddies from pole to pole.

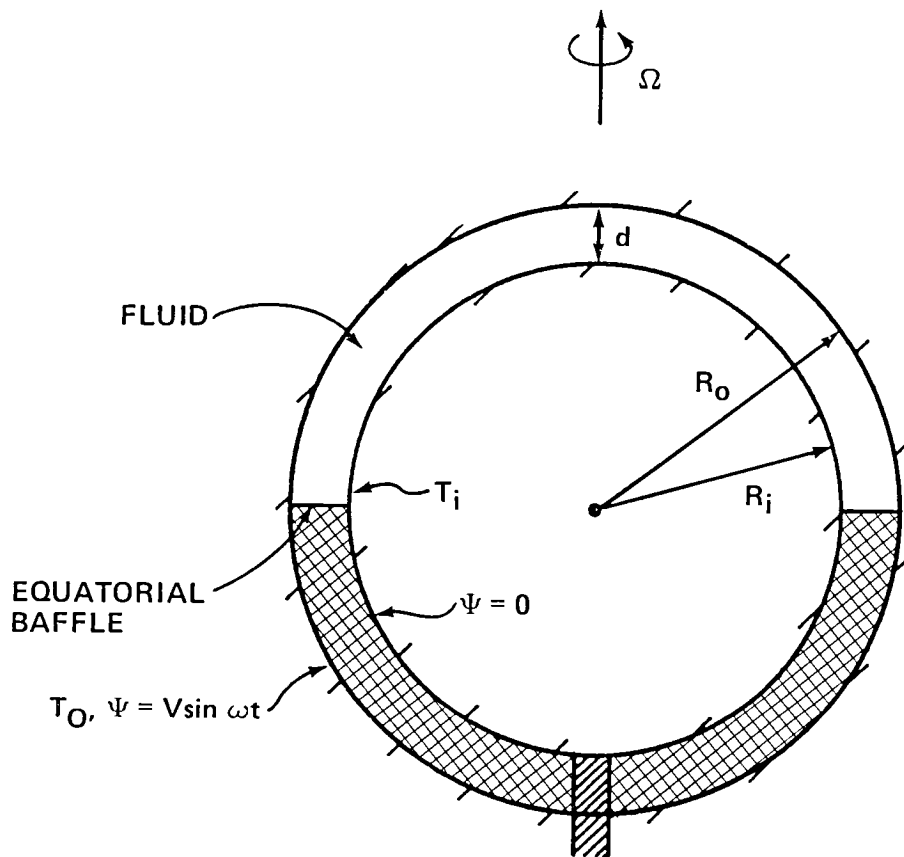
Theoretical models of planetary circulations indicate that the planetary curvature plays a crucial role in the dynamics of rotating atmospheres because the two major constraints on flow – rotation (Coriolis forces) and gravity (buoyancy forces) – vary with latitude relative to each other. Previous laboratory models of planetary atmospheres could not incorporate the curvature effect because, given the uniformity of terrestrial gravity, a rotating tank experiment was always required to have parallel rotation ( $\vec{\Omega}$ ) and gravity ( $\vec{g}$ ) vectors.

Simulation in the present experiment will be accomplished through the use of a dielectric fluid confined between concentric, rotating, electrically conductive spherical shells (Fig. III-1). The dielectric fluid will have a dielectric constant which is temperature dependent. Upon application of a voltage between the spheres, an electric field will occur; and a radially directed body force will act on the fluid in a manner exactly analogous to the gravitational body force which acts on oceans and stellar and planetary atmospheres. Because of the low-gravity environment of Spacelab, this experiment (unlike previous Earth-bound experiments) will contain the correct vector relationship between the rotation vector  $\vec{\Omega}$  and gravitational body force vector (per unit mass)  $\vec{g}$  of a planet; i.e.,  $\vec{\Omega} \times \vec{g} = \text{maximum value at equator}$  and  $\vec{\Omega} \times \vec{g} = 0$  at poles.

The apparatus includes a convection cell, temperature controllers for maintaining thermal boundary conditions at the inner and outer boundaries of the cell, a servo-controlled rotation drive to set the rotation speed, and a high-voltage supply (Fig. III-2). A camera is positioned above the cell at an angle to view a quadrant of approximately 90 degrees longitude and from equator to pole in the northern hemisphere. Visualization of the flow pattern is attained either by (1) injecting dye lines into the working fluid by exciting photochromic molecules and photographing the displacement of the dye or by (2) photographing the distortion of a set of ruled lines on the outer spherical shell caused by refractive index changes in the fluid. In either case, it will be possible to ascertain the state of the fluid – steady no-motion, steady axisymmetric, banded, unsteady, etc. In addition, the principal wavelengths and frequencies of the unstable modes will be measured.

Each experimental run is made with the rotation ( $\vec{\Omega}$ ) and applied voltage fixed, while the applied temperature difference  $\Delta T$  is raised slowly past a critical value which distinguishes simple axisymmetric unicellular motion from a more complicated state which may include banding or traveling waves. The nature of the instability for various thermal boundary conditions (constant temperature on inner and outer boundaries or meridionally varying temperature on inner boundary) will be determined. Of particular interest is the generation of mean zonally averaged flows by the eddies and any characteristic difference in the eddy structure between polar and equatorial regions.

The geophysical fluid flow cell experiment will permit the laboratory study in space of the large, planetary-scale dynamics of the Earth's oceans and atmosphere. The experiment should be able to verify existing theories of moderately nonlinear fluid systems on spherical surfaces and provide basic data on flows which are more strongly nonlinear than can currently be handled on a computer or by asymptotic methods. Of particular interest is the orientation of flow instabilities at various external conditions.



THE OUTER SHELL AT RADIUS  $R_o$  IS MAINTAINED AT TEMPERATURE  $T_o$ , VOLTAGE  $\psi = 0$ . THE INNER SHELL AT RADIUS  $R_i$  IS AT TEMPERATURE  $T_i$ , VOLTAGE  $V \sin \omega t$ . THE APPLIED FREQUENCY IS 60 Hz. THE TEMPERATURE DIFFERENCE  $\Delta T = T_i - T_o (> 0$  FOR UNSTABLE CONVECTION). THE ENTIRE APPARATUS IS ROTATED ABOUT ITS AXIS. THE INTERIOR IS FED VIA A SUPPORTING NECK.

Figure III-1. Geometry of the GFFC rotating spherical shell experiment.



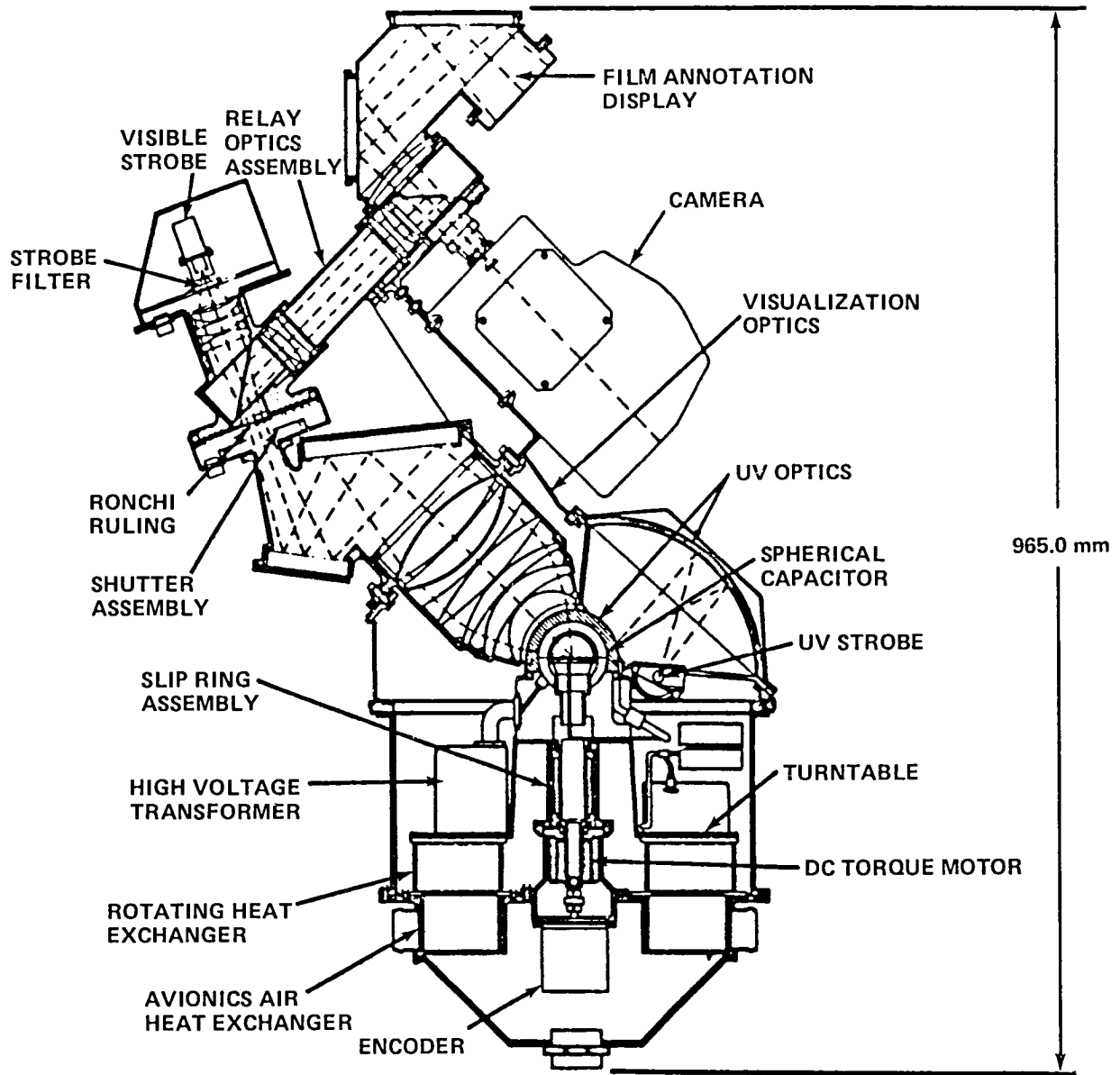


Figure III-2. Geophysical fluid flow cell.



## IV. AMES RESEARCH CENTER LIFE SCIENCES PAYLOAD

Paul X. Callahan  
John W. Tremor  
NASA Ames Research Center

### A. RESEARCH ANIMAL HOLDING FACILITY – VERIFICATION TEST (RAHF-VT)

In response to a recognized need for an in-flight animal housing facility to support Spacelab life sciences investigators, a rack- and system-compatible Research Animal Holding Facility (RAHF) has been developed. A series of ground tests is planned to insure its satisfactory performance under certain simulated conditions of flight exposure and use. However, even under the best conditions of simulation, confidence gained in ground testing will not approach that resulting from actual spaceflight operation. The Spacelab Mission 3 provides an opportunity to perform an inflight Verification Test (VT) of the RAHF. Lessons learned from the RAHF-VT and baseline performance data will be invaluable in preparation for subsequent dedicated life sciences missions.

The RAHF is configured to support animals ranging in size from rodents to small primates by cage module interchange. It is predicated that such a system will satisfy the experimental requirements of the great majority of prospective investigators working with commonly used laboratory mammals. This assumption has been validated to date by the experiments proposed and currently supported for the dedicated life sciences Spacelab (Spacelab 4).

The RAHF planned-for flight on Spacelab 3 comprises two major units: (1) an Ames Single Rack (ASR) containing 4 monkeys and (2) an Ames Double Rack (ADR) containing 24 rats and ancillary equipment (Fig. IV-1). Over the 7-day flight, food and water dispensed will be automatically monitored. A photocell method will be used to record animal activity intensity and pattern. The four monkeys and four of the rats will be monitored, by biotelemetry, for deep body temperature and heart rate and waveform. Four rats will be intermittently photographed during the mission by a movie camera programmed at given frame rates to assess behavioral response to launch/recovery conditions and to weightlessness. Housekeeping data will include RAHF temperatures and relative humidity.

RAHF-VT biocompatibility will be assessed after the flight by measurements of weight, growth, appearance, pathology, and behavior. Rodent histology, body composition, hormone and mineral levels, and vestibular morphology will be determined as well.

Influencing flight environment factors will be taken into consideration in interpretation of RAHF performance and biological response. These will include ambient temperatures, atmospheric composition, and flight dynamics.

A Dynamic Environment Measurement System (DEMS) is planned to accompany the RAHF and will yield acceleration, vibration, and noise data through launch and re-entry. Such information will be important in designing postflight control studies and developing subsequent experiments.

In addition to preflight testing, baseline information will be obtained from flight-simultaneous ground controls maintained in flight-similar hardware and conventional caging systems in a ground laboratory.

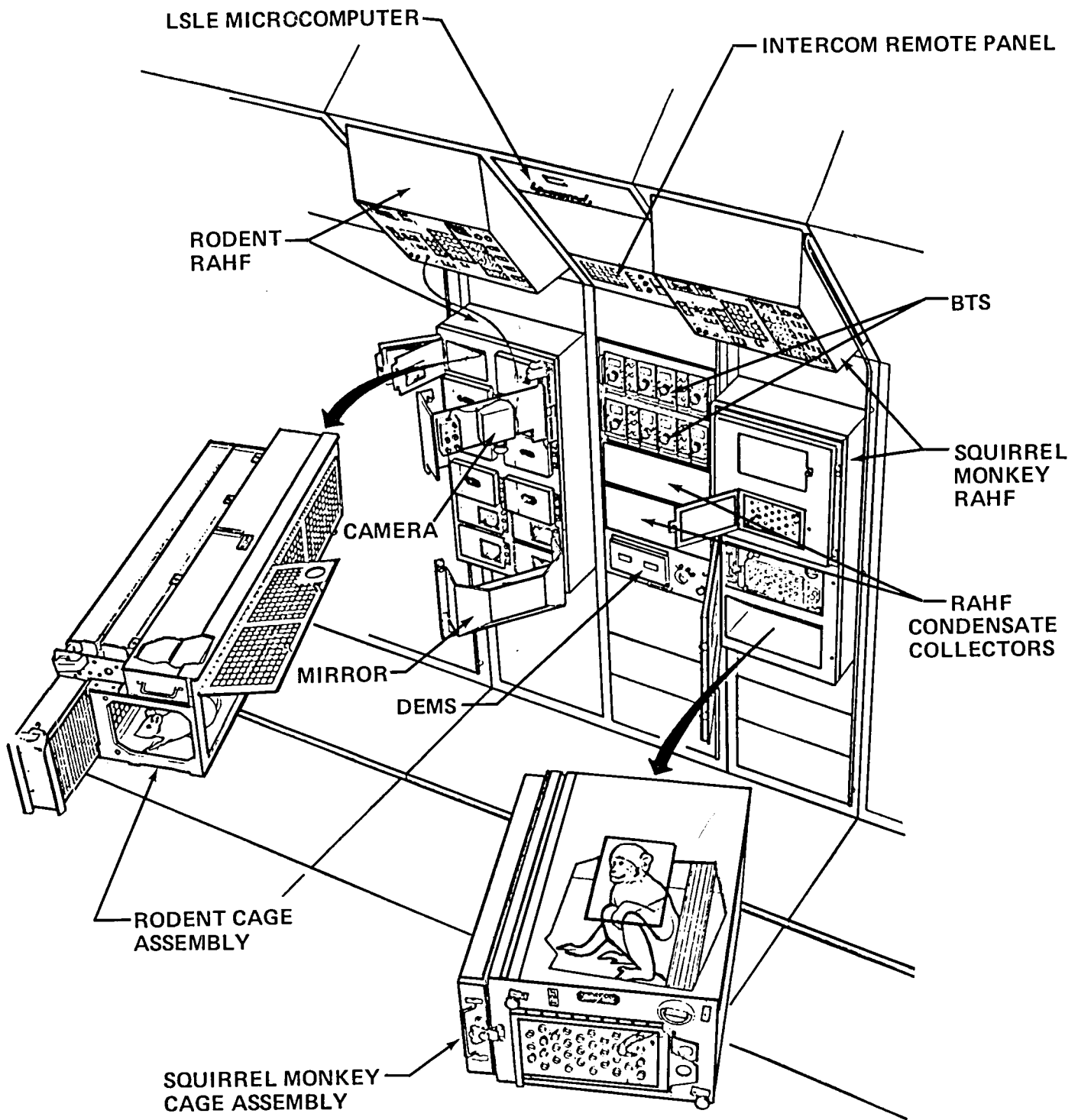


Figure IV-1. Ames double rack (ADR) and Ames single rack (ASR); representation of RAHF-VT, DEMS, and BTS.

As soon as possible after flight, data will be analyzed and made available to the community, in particular to those involved in preparations for the dedicated life sciences missions. The hardware will be refurbished and corrections made, where determined necessary and feasible, in operating procedures and hardware systems.

The success of the Spacelab 3 RAHF-VT will be measured by various standards. The basis of evaluation for engineering purposes will be performance of the following subsystems: cages and cage modules; environmental control; food delivery; water delivery; lighting; activity monitors; waste management; data; controls and displays; and, as it satisfies the interfaces among the craft, crew and ground systems.

Much of the information concerning the interfaces and performance of the RAHF will come from first-hand observations of those working with the RAHF and from the data obtained during pre-integration checkout, integration, late access animal loading operations and launch, in-orbit operation, and postflight early access animal retrieval and hardware checkout.

Biocompatibility of the specimens/RAHF system as influenced by the Spacelab 3 operational sequencing and flight profile will be determined principally by comparison of baseline and ground data gathered under simulated flight conditions with the flight-generated data and postflight analysis noted previously. Insofar as possible, differences in effect between the severe and complicating launch/re-entry environments and low inflight gravity levels will be determined by preflight, simultaneous, and, if necessary, postflight simulations. The basic question to be answered here is: Are there any peculiarities of space flight operations that affect the RAHF capability of supporting its contained specimens?

The Spacelab 3 RAHF-VT will also serve as an important experience for the many supporting engineers and scientists in preparing for the following dedicated life sciences missions. Although not directly related to the assessment of RAHF-VT, some of the data obtained may suggest useful scientific areas to probe on future missions and may aid in the design of such experiments.

## B. DYNAMIC ENVIRONMENT MEASUREMENT SYSTEM AND BIOTELEMETRY SYSTEM INVESTIGATIONS

The objective of both these investigations is to verify the performance of the prototype Dynamic Environment Measurement System (DEMS) and Biotelemetry System (BTS) equipment and techniques. The primary application of both systems will be to provide supporting data for interpreting and assembling the results of the Ames Research Animal Holding Facility (RAHF) verification test (Fig. IV-1). The DEMS is designed to measure noise, vibration, and acceleration forces. The unit is mounted in rack 7 between the two RAHF units. The BTS is designed to measure basic physiological functions in experimental animals. In the case of the Spacelab 3 mission, the unit is designed to measure the deep body temperature and heart rate and ECG pattern for four squirrel monkeys and four rats which will be contained in the RAHF's. The sensors and transmitter package are implanted in the animals preflight. Sensors data are telemetered to an antenna within the RAHF cages and routed to the BTS through antenna lead-in cables from both RAHF's.

The crew activities associated with these investigations include activation, monitoring, and periodic adjustment of the instrument operation. Both the DEMS and the BTS utilize Spacelab power. The BTS uses a dedicated Life Sciences Laboratory Equipment (LSLE) microcomputer to telemeter data to the ground during its continuous operation throughout the on-orbit phase of the mission. The BTS is operational only during this on-orbit phase. During ascent and descent, the DEMS stores the data in a tape recorder mounted on the front panel. The DEMS and data recorder are crew activated just prior to launch through a switch, and data are automatically recorded until Spacelab activation.

Upon Spacelab activation, the crewmember switches the DEMS off and the BTS to Spacelab power/data transmission mode. Power to the BTS is verified by front panel displays. The LSLE microcomputer is reset by a front panel switch. The signal strengths for the BTS are then adjusted using front panel controls/displays. This latter operation is performed periodically, and may be requested by ground operations at other times. The data and signal strengths are monitored and verified at the Science Monitoring Area (SMA) concurrently with inflight operations. Prior to Spacelab deactivation, the BTS is deactivated; the tape cassette in the data recorder is changed out; and the DEMS is switched to the descent mode through front panel controls. DEMS data are automatically recorded during the Spacelab re-entry phase.

In future dedicated missions, the DEMS will be useful to experiments where indices of external environmental factors (noise, vibration) must be taken into account in both the performance of tests and the interpretation of results. The concept of the BTS is likewise anticipated to support follow-on life sciences experiments which make use of experimental animals by providing the important capability of monitoring specimen body temperature and other basic physiological functions such as cardiac activity (ECG) and muscular activity (EMG).

## V. JSC LIFE SCIENCES PAYLOAD

### URINE MONITORING INVESTIGATION

Howard Schneider  
NASA/Johnson Space Center

The SL-3 JSC Life Sciences Payload consists of the Urine Monitoring Investigation. The hardware associated with this investigation is located in the Orbiter middeck. Interfaces within the middeck consist of the stowage of several hardware items in the middeck lockers and the temporary mounting of equipment during operations.

The primary objectives of the Urine Monitoring Investigation are: (1) to verify the operation of the Urine Monitoring System (UMS) in the collection and sampling of urine, (2) to perform inflight measurement calibration of the UMS, (3) to develop and utilize a feasible procedure for monitoring crew water intake using the existing galley water supply and Shuttle food system, and (4) to verify the system for preparing urine samples for postflight analysis. Subsequent dedicated life sciences missions are anticipated to incorporate the UMS in support of a number of experiments which will be directed at studying the body volume disturbances which result from low-gravity exposure. The data from the urine volume measurements and, particularly, from the analysis of samples collected during the Spacelab 3 inflight operational performance of the UMS will help extend the present understanding of the adaptive changes which alter the fluid, electrolyte, renal, and circulatory status of humans exposed to the weightless environment of space flight. The proposed measurements on the collected urine samples include indices of renal function and electrolyte, protein, and hormone levels. The results will provide insight into the fluid redistribution hypothesis which has been proposed to account for circulatory-endocrine-renal involvement in the loss of fluids and electrolytes during the immediate inflight period, and it will extend the Skylab observations in the adapting phase of flight by examining specific urine biochemical parameters related to the development of new homeostatic levels. Limitations of previous space flight studies will be overcome by ensuring that subjects are adequately hydrated, by performing urine collection on a void-by-void basis, by collecting data early in flight, and by monitoring crew water intake throughout the mission.

The Urine Monitoring Investigation is designed to evaluate the UMS and monitor the water intake of the crew. The UMS consists of the UMS assembly and sample container assembly (Fig. V-1). Designed as a carry-on unit capable of accommodating eight crewpersons, it will be stowed in Orbiter middeck lockers (Fig. V-2) for launch and return and installed inflight in the Orbiter middeck near the Orbiter waste collection system. The operations associated with this investigation include: crew water intake monitoring, crew urine collection and sampling, and measurement calibration. The water intake monitoring portion of the investigation requires that each crew person record the daily drinking water consumption; non-menu beverage or food consumption; menu items not consumed; pantry items substituted for menu items; and an estimate of amount consumed, in the event of partial consumption.

The urine collection and sampling portion of this investigation requires urine volume measurement on a void-by-void basis on all crew persons and urine sampling on two crew persons. The urine measurement activities require that the UMS assembly and sample container assembly be removed from the middeck stowage locker and installed in the Orbiter middeck near the WCS. The UMS flush water inlet is connected to the galley water supply, and the UMS power connection is made to an Orbiter service outlet. The sample container assembly is maintained in the WCS compartment near the UMS. In this configuration, the UMS assembly is in a standby mode and remains in this configuration throughout the flight. Urine collection will be performed automatically in each urine void. Urine sampling will be accomplished by the UMS in the sampling mode. Sample containers are removed from the UMS and stored in the sample container assembly.

The measurement calibration portion of this investigation will be accomplished by comparing the UMS volume measurements to premeasured aliquots of water containing salt (specific gravity 1.021). The premeasured aliquots will be launched in 32 modified, veterinary dose, 300-ml syringes and injected into the urinal during flight. The syringes will be utilized in different groupings to provide a range of calibration volumes resulting in 20 data points. Following injection, the UMS dump cycle will be activated, as during normal micturition. The syringes will be recapped and returned to Earth to allow measurement of and correction for the residual fluid.

Deactivation activities for this investigation consist of deactivating the UMS assembly upon completion of the urine collection and sampling operation as late in the mission as possible. The UMS assembly and other associated hardware are then stowed in the Orbiter middeck lockers for return.

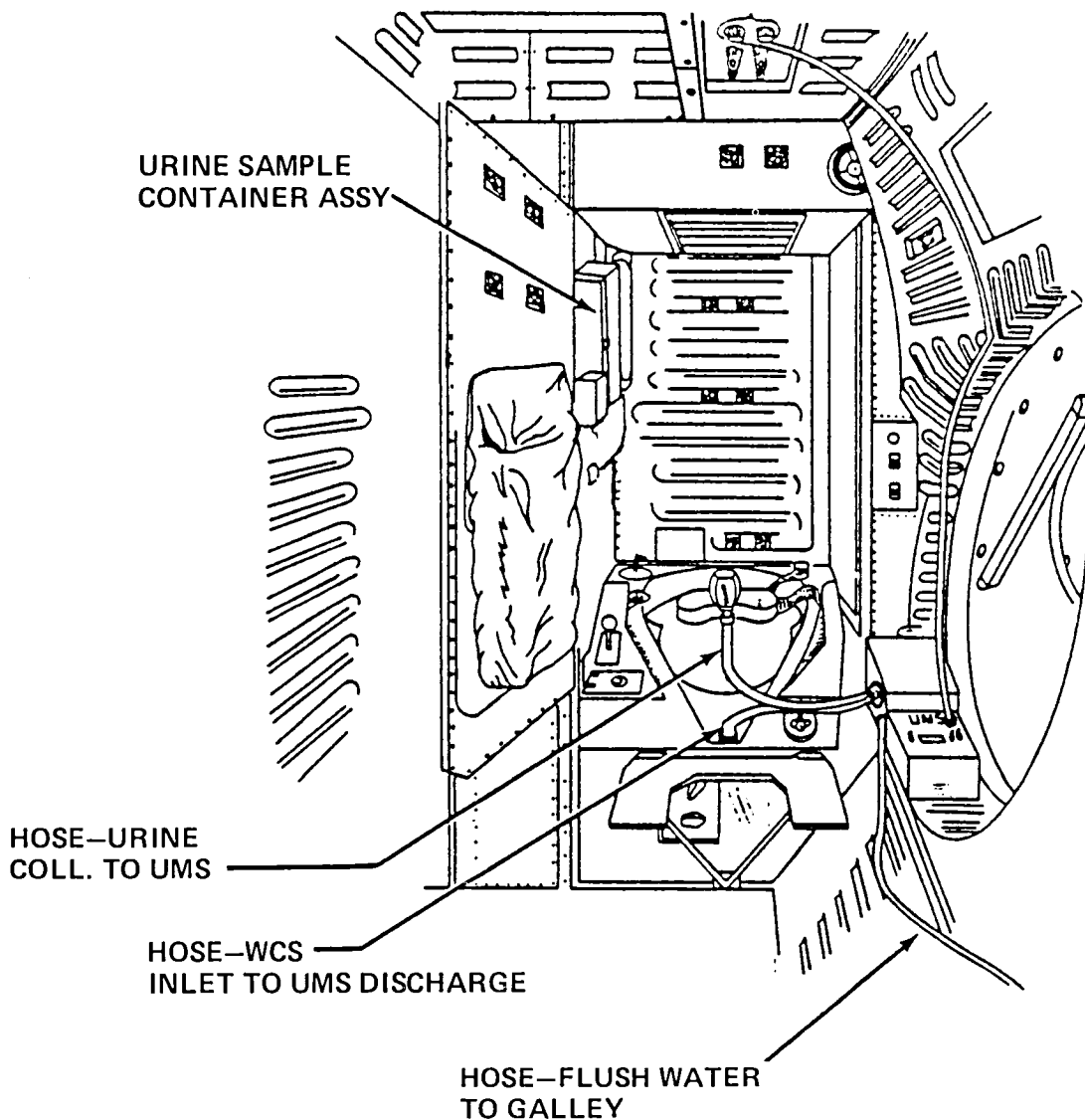


Figure V-1. Urine monitoring system on-orbit configuration.



## EXPERIMENT SUPPORT STRUCTURE EXPERIMENTS



## VI. ATMOSPHERIC TRACE MOLECULE SPECTROSCOPY

C. B. Farmer  
Jet Propulsion Laboratory

The Spacelab investigation entitled Atmospheric Trace Molecule Spectroscopy (ATMOS) is designed to obtain fundamental information related to the chemistry and physics of the Earth's upper atmosphere using the techniques of infrared absorption spectroscopy. There are two principal objectives to be met. The first is the determination, on a global scale, of the compositional structure of the upper atmosphere and its spatial variability. The establishment of this variability represents the first step toward determining the characteristic residence times for the upper atmospheric constituents; the magnitudes of their sources and sinks; and, ultimately, an understanding of their effects on the stability of the stratosphere. The second objective is to provide the high-resolution, calibrated spectral information which is essential for the detailed design of advanced instrumentation for subsequent global monitoring of specific species found to be critical to atmospheric stability. This information will be disseminated in the form of a three-dimensional atlas of solar absorption spectra obtained over a range of latitudes, longitudes, and altitudes.

The spectra which will be acquired in the course of the ATMOS investigation will contain, in addition to the compositional data described previously, a great deal of information related to the physics of the upper atmosphere. For example, the data obtained will also make it possible to describe the three-dimensional temperature structure and to study local departures from thermodynamic equilibrium regimes of dissociation as well as radiative transfer processes. Investigators with special interests in each of these areas have been included in the ATMOS science team to insure that the instrument and experiment, as finally designed, will be capable of making the necessary measurements.

The choice of the remote sensing method for acquiring the data is dictated by the need to obtain simultaneous concentration information for a large number of stratospheric species in times sufficiently short to provide useful spatial resolution. The one common characteristic possessed by almost all of the species of interest is that their rotational and vibrational transition frequencies lie in the infrared region; and, thus, simultaneous measurements can be made using infrared spectroscopic techniques. However, the transition frequencies are widely separated from different constituents, necessitating broad wavelength coverage in each observation. Moreover, in adopting the solar absorption mode as the experimental technique to be used from Spacelab, each observation must be made in times on the order of 1 to 2 sec if the required vertical resolution is to be obtained. Interferometry, with its high-energy throughput and multiplexing advantages, is the only infrared technique capable of satisfying these last two constraints. The ATMOS instrument will thus be a continuous-scanning Fourier spectrometer operating in the 2- to 16- $\mu\text{m}$  wavelength region and capable of generating one interferogram each second with a spectral resolution of 0.01  $\text{cm}^{-1}$ . The characteristics of the instrument are summarized in Table VI-1.

The ATMOS instrument is comprised of four major elements: a suntracker, a telescope, an interferometer, and a data handling system. A schematic of the optical layout is shown in Figure VI-1. The suntracker contains two single-axis, motor-driven mirrors and a silicon diode assembly for sensing and controlling the position of the mirrors with respect to the Sun. A 16 mm camera records the Sun superimposed over the field stop to verify the position of the pointing vector with respect to the solar disc during each observation. An  $f/2$  telescope system is used to concentrate the radiation received into a beam suitable for the interferometer. Cat's-eye retroreflectors replace the plane mirrors used in a conventional Michelson interferometer. A retroreflecting mirror double passes the radiation through the arms of the interferometer before it is recombined and sent to the detector. The use of the cat's-eye retroreflectors and double passing make the instrument insensitive to both angular and lateral motion of the moving elements. The detector

is a HgCdTe type, cooled to cryogenic temperatures. Its output is amplified and digitized by the data-handling system and multiplexed with the optical path difference information and housekeeping data into a single 15.7 megabit/sec data system. A system controller, which coordinates all instrument functions and operations, formats the data for proper telemetry inputs and provides a responsive interface to the instrument microprocessor. Data-taking sequences are normally initiated by pre-entered command.

The experimental approach for acquiring the necessary data from Spacelab will be to view the Sun with the ATMOS instrument during the periods just prior to entry into, and shortly after emerging from, solar occultation; specifically, the viewing periods will be timed to occur when the ATMOS instrument's view of the Sun is being occulted by the upper atmosphere. During these periods, the instrument will make a set of interferometric measurements of the solar radiation incident upon it as a function of optical path difference within the instrument. This observational method is illustrated in Figure VI-2. Subsequent transformation of these measurements utilizing a specialized Fourier transform technique will produce spectra of the solar continuum between 2 and 16  $\mu\text{m}$  with the characteristic absorption features of all the stratospheric and mesospheric species present superimposed upon it. Each set of measurements, generated for stratospheric layers at different altitudes, will provide the information necessary to establish vertical composition profiles for the species of interest.

Because of data rate and instrument performance considerations, the entire spectral region from 2 to 16  $\mu\text{m}$  will not be covered in a single scan, but will be divided instead into narrower wavelength intervals by the use of optical filters. The ATMOS instrument has been designed with provisions for six such filters. The bandpass for each is shown in Table VI-2, together with a list of those important minor and trace upper atmospheric species whose most favorable transition frequencies lie within each spectral interval. Although performance and data rate considerations also constrained the choice of bandpasses for the filters shown in the table, it is apparent that measurements of almost all of the species of current interest can be made in the regions encompassed by filters 1 and 3. The expected detectability as a function of altitude for each of the species listed in Table VI-2 is shown in Figure VI-3.

The geographical spread of the data which will be obtained from the ATMOS experiment is determined by the orbital geometry associated with the Spacelab launch conditions. Seventy-two (72) observations are planned for the ATMOS experiment, approximately half of them sunrises and the other half sunsets. Sunrises or sunsets should occur in the latitude band of  $\pm 15$  degrees, centered on the subsolar latitude at the time of the flight.

During each of the 72 occultations, the ATMOS instrument will have a 3-min period of operational time in which to acquire a data set. The ATMOS Science Team is planning the filter sequencing for each occultation to insure that all of the spectra are acquired which are needed to meet the primary and secondary objectives of the experiment. Preliminary estimates indicate that a data set may include as many as 100 interferograms.

The ATMOS data stream will be multiplexed into the general data stream from Spacelab and transmitted via satellite in real time to the Goddard Space Flight Center for demultiplexing and preliminary formatting. All other aspects of the data reduction will be accomplished on a dedicated facility at the Jet Propulsion Laboratory. The facility will consist of a minicomputer and fast array processor with two interactive consoles, two tape drives, and two 300-megabit disc drives. In addition to the program used for data reduction, the software package for the ATMOS facility will contain relatively complex programs for interactive analysis of the data, including algorithms for measuring and comparing equivalent widths and for generating synthetic spectra for comparison with the observed data. The ATMOS investigators will be able to use this interactive capability; or, alternatively, they may request hard copy or tape of the spectra in their regions of interest for analysis at their own facilities.

TABLE VI-1. ATMOS INSTRUMENT CHARACTERISTICS

|   |
|---|
| <p>Experiment Design Criterion: 2 km spatial resolution.</p> <p>Field of view: <math>1 \times 10^{-3}</math> or <math>2 \times 10^{-3}</math> rad, selectable</p> <p>Aperture: 45 mm, circular</p> <p>Scan time: 1 second per interferogram</p> <p>Experiment Spectral Criteria:</p> <p>Wavelength (frequency) coverage: 2 to 16 <math>\mu\text{m}</math> (5000 to 625 <math>\text{cm}^{-1}</math>)</p> <p>Resolution: 0.01 <math>\text{cm}^{-1}</math> (unapodized)</p> <p>Sun Tracker Parameters:</p> <p>Accuracy: <math>\pm 0.5 \times 10^{-3}</math> rad.</p> <p>Stability: <math>\pm 0.1 \times 10^{-3}</math> rad.</p> <p>Range: 120° elevation, 360° azimuth</p> <p>Unobstructed view angles: <math>\pm 120^\circ</math> about roll axis, <math>\pm 90^\circ</math> about pitch axis</p> <p>Interferometer Parameters:</p> <p>Type: Double-passed, parabolic cat's-eye, flatplate beam splitter.</p> <p>Beam Splitter Substrate: KBr</p> <p>Sampling Reference: 0.6328 <math>\mu\text{m}</math> HeNe laser</p> <p>Sampling Interval: 2 or 3 times reference wavelength</p> <p>Telescope Magnification: 2.6</p> <p>Optical Path Difference: 50 cm</p> <p>Detector Parameters:</p> <p>Type: HgCdTe</p> <p>Noise Equivalent Power (NEP): <math>5 \times 10^{-13}</math> watts at <math>\lambda_{\text{peak}}</math></p> <p>Time Constant: <math>&lt; 200 \times 10^{-9}</math> sec</p> <p>Data Handling System Parameters:</p> <p>Samples per Interferogram: <math>2.67 \times 10^5</math> or <math>4 \times 10^5</math></p> <p>Sampling Frequencies: <math>132 \times 10^3</math> or <math>198 \times 10^3</math> per sec</p> <p>Signal Frequencies: 31.3 to 250 kHz</p> <p>Data Rate: <math>15.7 \times 10^6</math> bits/sec</p> <p>Output: Serial NRZ, PCM</p> |
|---|

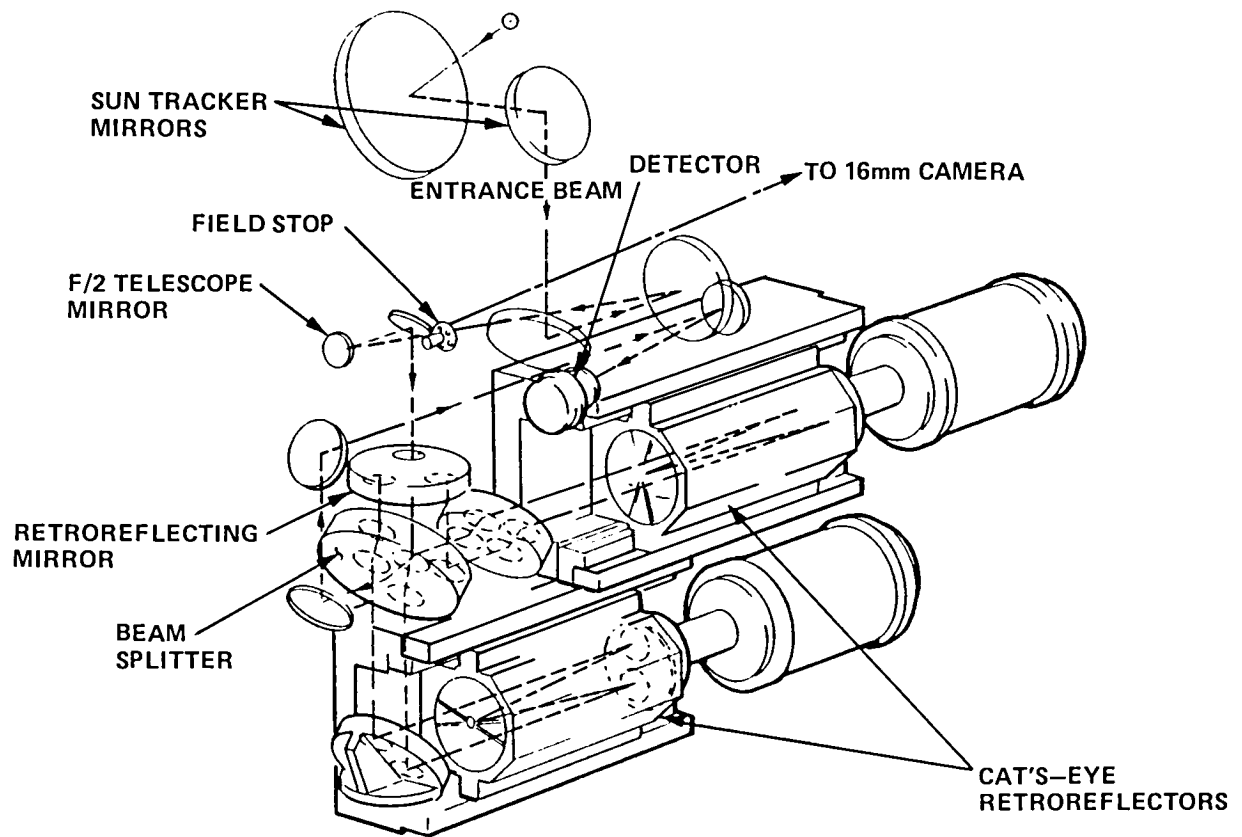


Figure VI-1. ATMOS: interferometer optical path.

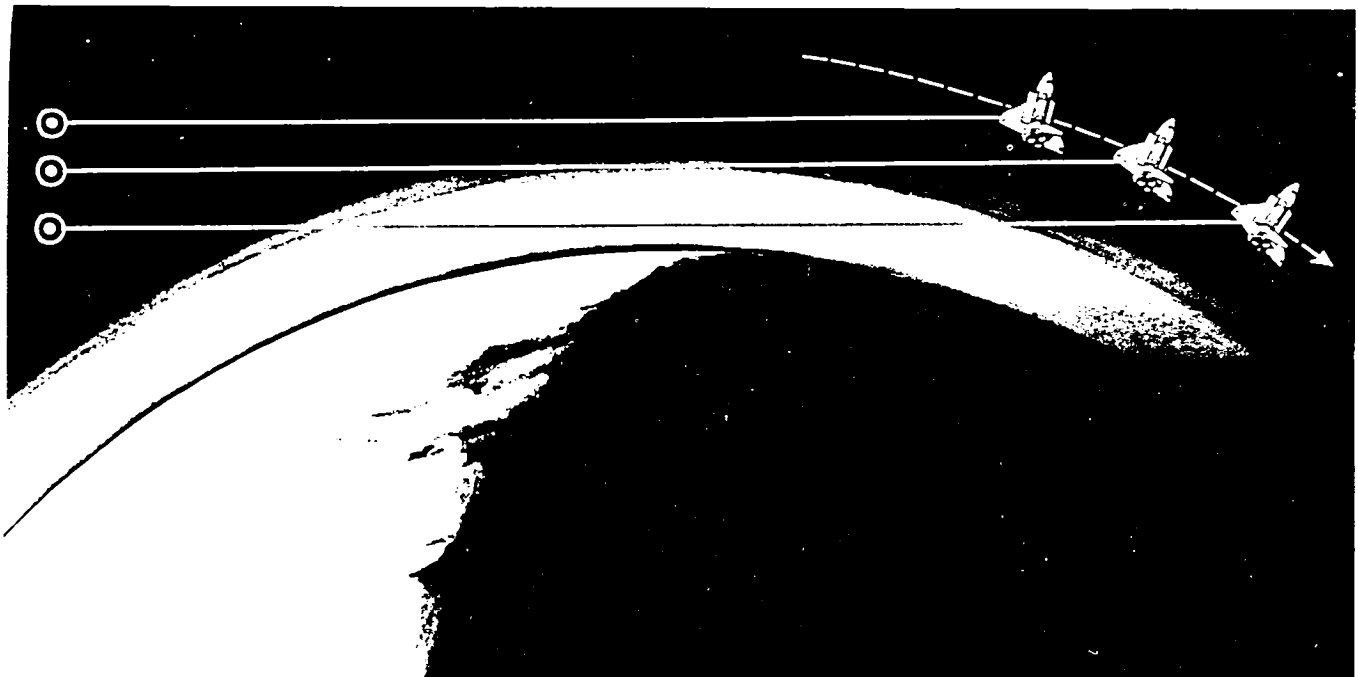


Figure VI-2. ATMOS observational method for a typical sunset occultation, showing the Orbiter as it views solar radiation [O] passing through successively lower layers of the stratosphere.

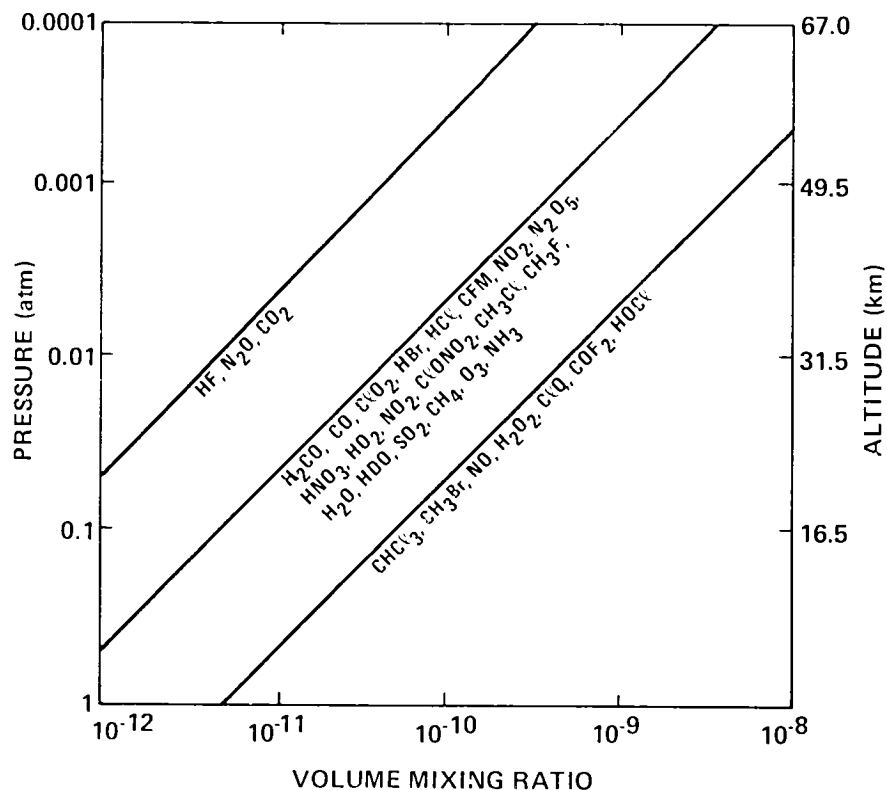


Figure VI-3. Expected detectability of several of the important stratospheric species by ATMOS.

TABLE VI-2. TRANSMISSION REGIONS FOR ATMOS OPTICAL FILTERS SHOWING PRINCIPAL SPECIES TO BE MEASURED

| A<br>600–1200 $\text{cm}^{-1}$  | B<br>1100–2000 $\text{cm}^{-1}$ | C<br>1580–3400 $\text{cm}^{-1}$ | D<br>3100–4400 $\text{cm}^{-1}$ |
|---------------------------------|---------------------------------|---------------------------------|---------------------------------|
| CFM                             | CH <sub>4</sub>                 | HCl                             | O <sub>3</sub>                  |
| ClONO <sub>2</sub>              | H <sub>2</sub> O                | HBr                             | CH <sub>4</sub>                 |
| CHCl <sub>3</sub>               | H <sub>2</sub> O <sub>2</sub>   | CH <sub>3</sub> Cl              | CO                              |
| NH <sub>3</sub>                 | SO <sub>2</sub>                 | CH <sub>3</sub> F               | CO <sub>2</sub>                 |
| HNO <sub>3</sub>                | CO <sub>2</sub>                 | CH <sub>3</sub> Br              | NO <sub>2</sub>                 |
| O <sub>3</sub>                  | COF <sub>2</sub>                | N <sub>2</sub> O                | H <sub>2</sub> O <sub>2</sub>   |
| ClO                             |                                 | H <sub>2</sub> CO               | ClO <sub>2</sub>                |
| N <sub>2</sub> O <sub>5</sub>   |                                 | HOCl                            | COF <sub>2</sub>                |
| HO <sub>2</sub> NO <sub>2</sub> |                                 | H <sub>2</sub> O                |                                 |
| SO <sub>2</sub>                 |                                 | HDO                             |                                 |
| CO <sub>2</sub>                 |                                 | NO                              |                                 |





## VII. STUDIES OF THE IONIZATION STATES OF SOLAR AND GALACTIC COSMIC RAY HEAVY NUCLEI

S. Biswas

Tata Institute of Fundamental Research, India

Cosmic ray nuclei of galactic origin have been studied during the past 20 years and energetic solar nuclei during the past 15 years in an attempt to understand the characteristics of their sources and the nature of their acceleration processes. Until recently, the chemical composition and energy spectra of these nuclei were determined only for energies equal to or greater than 50-million electron volts per atomic mass unit. Recent studies at lower energies indicate that the charge and energy distribution of low-energy cosmic rays are different from that of high-energy cosmic rays. Observations of the flux of medium nuclei (C, N, O) at 10-million electron volts per atomic mass unit appear to indicate that the nuclei may be partially ionized, in contrast to high-energy nuclei which are completely ionized; i.e., all electrons are stripped from the nucleus. The origin of this new component of cosmic rays is unknown.

Enhancement of abundances of heavy nuclei (e.g., Mg, Si, and Fe) at low energies relative to solar photospheric abundances and anomalously high abundances of iron relative to oxygen nuclei at low energies were recently discovered in solar energetic particles studied at low energy. These phenomena are not understood at present. It is believed that they are probably related to the partly ionized states and acceleration processes.

The proposed experiment is designed to study the recently discovered anomalous component of low-energy galactic cosmic ray ions of C, N, O, Ne, and Ca to Fe of energy 5- to 10-million electron volts per atomic mass unit in regard to their ionization states, composition, and intensity, and to study the ionization states of heavy elements from oxygen to iron in energetic solar particles emitted during flare events. The same detector system will serve for both studies, with the second objective being given priority if there are any solar particle events during the mission.

The detector system (Fig. VII-1) consists of stacks of thin sheets of special plastics such as cellulose nitrate (CN) and lexan polycarbonate, which are efficient low-noise detectors for heavy nuclei. The stacks are in the shape of a cylindrical module with a diameter of 40 cm and a height of approximately 5 cm. There are two distinct stacks, a major lower stack (5-cm thick) which is slowly rotated at the rate of 4 degrees/hr with respect to a thin, fixed upper stack (0.5-cm thick) with a separation of 0.05 cm.

An energetic particle entering through the top stack and stopping in the bottom stack leaves a damage trail along its path that can be revealed optically by a suitable chemical treatment in the laboratory. The identity and energy of the particle can then be determined from measurements on the geometry of the tracks and the range traversed in the stack. Also, by identifying the segments of the same track in the top and bottom stacks, the arrival time of the particle can be determined from the displacement between the segments. The arrival time can be measured to the nearest 20 sec in the present design; and this, coupled with the arrival direction, gives the lower bound on the magnetic rigidity (momentum/effective charge) of the particle as determined by the Earth's magnetic field configuration. Thus, the combined information permits the determination of the particle's charge state.

The structure housing consists of an approximately cylindrical enclosure of approximately 44-cm diameter and 25-cm height, the top of the enclosure being covered by a thin spherical shell of aluminum. Inside the housing, a high-resolution stepper motor rotates the lower detector stack with respect to the fixed upper one in steps of approximately 40 arc-sec once in 10 sec, so that full 360 degrees rotation is completed

in 90 hr. The rotation history of the detector stack is recorded and monitored with a 15-bit optical absolute shaft angle encoder. The instrument enclosure is maintained at one-tenth atmospheric pressure. The operation of the instrument is controlled by the on-board experiment computer through a Spacelab-provided remote acquisition unit. Thermal control of the instrument is provided by the pallet cold plate on which the instrument is mounted and by a reflective coating on the outer surface.

The information obtained is of two kinds. One, which is telemetered to the ground together with time and Spacelab attitude vectors, is the output of the angular motion of the shaft angle encoder. The other is the data obtained from the measurements on particle tracks in the detectors with optical microscopes. Analysis of these data is carried out for identifying nuclear charge and energy using an interactive program package employing graphic displays. Combining this information allows the determination of ionization states of solar and galactic cosmic ray heavy nuclei of 5- to 10-million electron volts per atomic mass unit energy.

The direct measurements of the charge state of low-energy heavy ions are crucial to the understanding of new particle phenomena observed by the present investigator on Skylab and by several investigators on other satellites. Information on the ionization states of solar heavy nuclei which may be provided by this experiment (depending on the occurrence of solar flares) is of immediate interest in the understanding of the acceleration and confinement of energetic nuclei in the Sun.

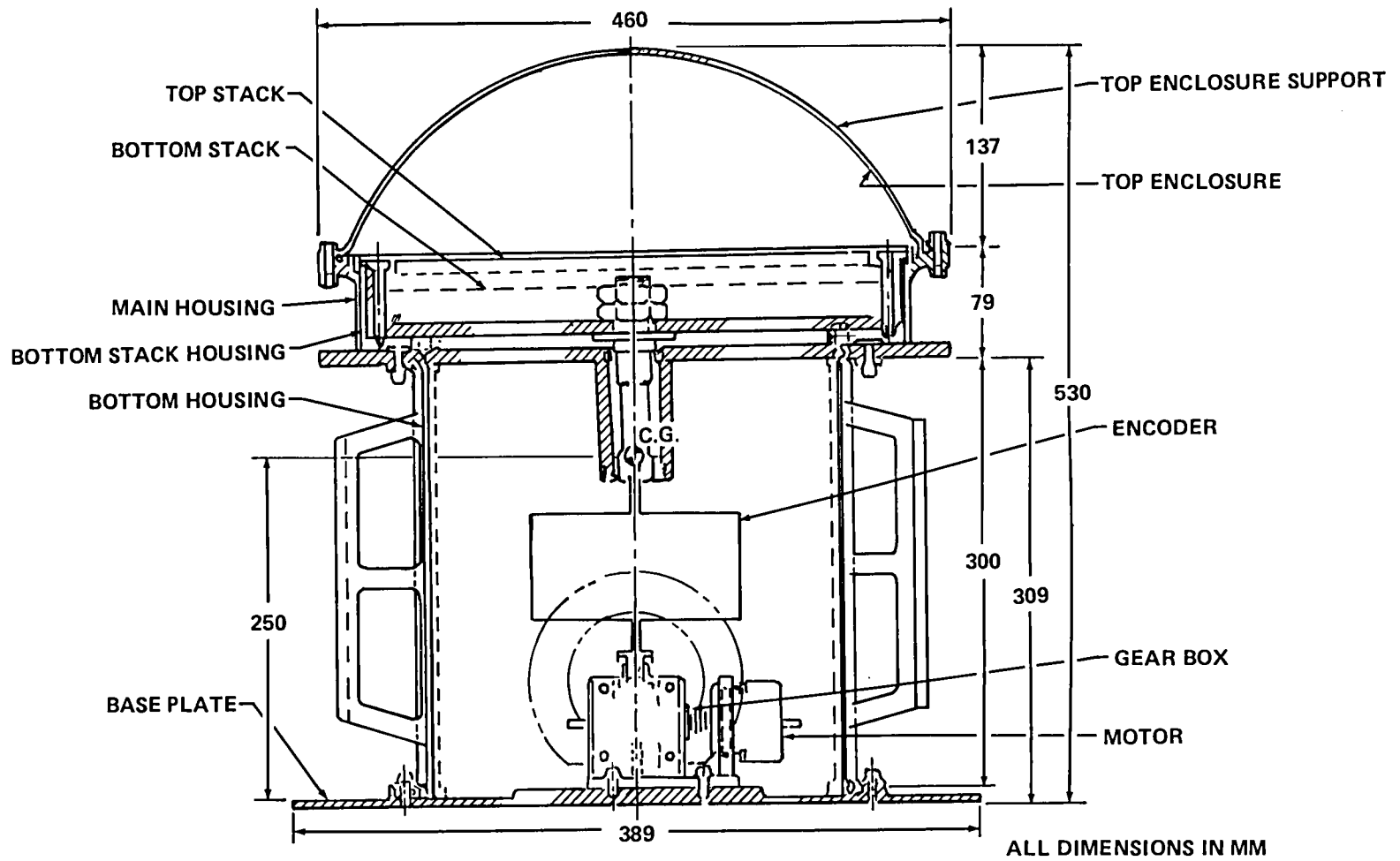


Figure VII-1. Sketch of the IONS (ANURADHA) detector assembly (sectional view).



## APPENDIX

### LIST OF CO-INVESTIGATORS

#### Module

##### FLUID EXPERIMENT SYSTEM (FES)

Dr. R. Kroes, NASA Marshall Space Flight Center

##### VAPOR CRYSTAL GROWTH SYSTEM (VCGS)

Dr. Lodewijk von den Berg, EG&G, Inc.

Dr. Michael M. Schieber, EG&G, Inc.

##### GEOPHYSICAL FLUID FLOW CELL (GFFC)

Dr. Juri Toomre, University of Colorado

Dr. Peter Gilman, National Center for Atmospheric Research

Dr. George H. Fichtl, NASA/MSFC

Dr. William Fowles, NASA/MSFC

Dr. Fred W. Leslie, NASA/MSFC

#### Experiment Support Structure

##### ATMOSPHERIC TRACE MOLECULES SPECTROSCOPY (ATMOS)

Mr. Odell Raper, JPL

Dr. Robert Norton, JPL

Dr. Reinhard Beer, JPL

Dr. Fred Taylor, England

Dr. Moustafa Chahine, JPL

Dr. Robert Toth, JPL

Mr. Rudolf Schindler, JPL

Dr. James Breckinridge, JPL

Dr. John Shaw, The Ohio State University

Dr. Joel Susskind, NASA/GSFC

Dr. James Russell, NASA/LaRC


Dr. Rudolphe Zander, University of Liege

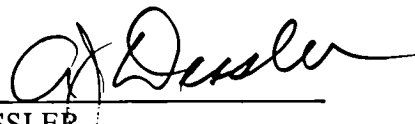
APPROVAL

SPACELAB MISSION 3 EXPERIMENT DESCRIPTIONS

Edited by C. Kelly Hill

The information in this report has been reviewed for technical content. Review of any information concerning Department of Defense or nuclear energy activities or programs has been made by the MSFC Security Classification Officer. This report, in its entirety, has been determined to be unclassified.

  
WILLIAM W. VAUGHAN  
Chief, Atmospheric Sciences Division

  
A. J. DESSLER  
Director, Space Sciences Laboratory



LANGLEY RESEARCH CENTER



3 1176 00517 7697